Doctor's Thesis : 0481202

Functional analysis of ATPase associated with various cellular activities (AAA) protein in tobacco plants

Mi-Hyun Lee

Research and Education Center for Genetic Information

Graduated School of Biological Sciences

Nara Institute of Science and Technology

(Professor Sano Hiroshi)

Submitted on 29th January, 2007

ABSTRACT

We previously identified a tobacco gene encoding an ATPase associated with various cellular activities (AAA) protein, which is involved in pathogen response, and designated as NtAAA1. In this study, I focused on its characterization at molecular and physiological levels, and found that it functions as a powerful attenuator of the hypersensitive response (HR) during pathogen infection.

In chapter I, using transgenic *NtAAA1*-RNAi tobacco plants, I performed differential micro-array screening to identify genes that were regulated by NtAAA1. In RNAi transgenic plants, genes related to salicylic acid (SA) were up-regulated, whereas those related to jasmonic acid (JA) and ethylene were generally down-regulated. When SA was exogenously applied to leaves, expression of pathogen responsive genes was evidently induced at much higher level in *NtAAA1*-RNAi transgenic lines than in the control. Simultaneous application of JA with SA cancelled the effect of SA, suggesting that NtAAA1 functions in response to JA and/or ethylene signals, resulting in interference with SA signaling pathways.

In chapter II, I searched for NtAAA1-interacting proteins by the yeast two-hybrid screening, and identified one particular gene encoding a small GTPase, an ADP

ribosylation factor designated as NtARF. Its specific interaction with NtAAA1 was confirmed by *in vitro* pull-down and FRET assays, and their interaction was predominant between active forms of NtARF and NtAAA1, each bound to GTP and ATP, respectively. Transgenic tobacco plants constitutively expressing *NtARF* under the control of the CaMV 35*S* promoter exhibited spontaneous and wound-induced lesion formation and enhanced resistance to pathogen attack. Expression of *NtAAA1* in leaves of NtARF transgenic plants attenuated lesion development and suppressed excess pathogen resistance. These observations indicate that NtAAA1 interferes with NtARF, which positively functions in resistance against pathogen attack. Transcripts of *NtAAA1* and *NtARF* were induced by ethylene and SA in wild type tobacco plants, respectively. Antagonistic actions of JA and/or ethylene and SA in defense response has long been documents, but its molecular basis was not clear. The NtAAA1/NtARF system may partly be responsible for it.

In conclusion, this study revealed that NtAAA1 specifically interacts with an ARF protein and reduces its function. I propose that defense reactions are concertedly regulated by fine balancing between enhancement and attenuation of the HR by various proteins, including the presently described NtARF and NtAAA1.

TABLE OF CONTENTS

Abbreviations

CFP	cyan fluorescent protein
DAB	3,3'-diaminobenzidine
DTT	(±)-dithiothreitol
EDTA	ethylene diamine tetraacetic acid
FRET	fluorescence resonance energy transfer
GFP	green fluorescent protein
GST	glutathione *S*-transferase
HR	hypersensitive response
IPTG	isopropyl β-D-thiogalactopyranoside
JA	jasmonic acid
$MgCl_2$	magnesium chloride
$MgSO_4$	magnesium sulfate
MOPS	3-(*N-morpholino*) propane sulfonic acid
PR	pathogenesis-related
SA	salicylic acid
SDS	sodium dodecyl sulfated
SCS	sodium chloride/sodium cirate
x-gal	5-bromo-4-chloro-3-indolyl- α-D-galactopyranoside
YFP	yellow fluorescent protein

Introduction

Plant stress response

Plants have developed the defense system by specifically recognizing pathogens and preparing protecting activities against their attack (Baker et al., 1997). These responses include production of reactive oxygen intermediates (ROI), strengthening of cell walls, synthesis of phytoalexins, and induction of pathogenesis-related (PR) proteins (Hammond-Kosack and Jones, 1996; Yang et al., 1997). In particular, hypersensitive response (HR) plays an important role in pathogen-response, as defined early and rapid programmed cell death (Goodman and Novacky, 1994). In addition to the HR, nonspecific immunity to infection by a variety of pathogens plays a critical role in defense reactions, this being known as systemic acquired resistance (Ryals et al., 1996).

In defense response, signal pathways are defined by the signaling molecules they produce and respond to, including jasmonic acid (JA), salicylic acid (SA), auxin and ethylene, synergistically or antagonistically function. JA is usually associated with wounding pathways, whereas SA is usually involved in pathogen responses (Felton and Korth, 2000). In many cases, SA is first associated with induction of pathogenesis-related (PR) proteins and subsequent establishment of systemic acquired resistance (SAR) (Ryals et al., 1996). SA also contributes to the HR-associated resistance (Delaney et al., 1994; Mur et al., 1997, 2000) via

mechanisms that produce reactive oxygene species (ROI) and cell death (Shirasu et al., 1997). JA and ethylene have been suggested to be important to modulate disease-resistance pathways that operate independently of SA (Pieterse and van Loon, 1999). SA-dependent and JA/ethylene-dependent pathways induce expression of different sets of PR genes, resulting in diverse resistance to different pathogens (Glazebrook, 1999; Wang et al., 2002). SA- and JA/ethylene-dependent pathway are not linear, can be established network of cross-talking connections that appear to co-ordinate responses (Devoto and Turner, 2003). Recent evidence indicates that antagonism between SA- and JA/ethylene pathway in plant defenses (Dares et al., 1995; Felton et al., 1999). For example, disrupt SA-mediated responses sensitized JA/ethylene pathway (Clarke et al., 1998, 2000; Gupta et al., 2000), indicating that SA may have an inhibitory effect on JA/ethylene biosynthesis or signaling (Jirage et al., 2001). Similarity, JA/ethylene can repress expression of SA-induced genes by inhibiting SA accumulation (Petersen et al., 2000). However, switch-on and -off mechanisms of the HR and systemic acquired resistance, and roles of phytohormones, have yet to be completely elucidated.

AAA protein: Its roles, structure and regulation

During the search for pathogen-responsive genes in tobacco plants, we identified a particular example encoding an ATPase associated with a various cellular activities (AAA)

protein which appeared to reduce the HR upon tobacco mosaic virus infection and was designated as NtAAA1 (Sugimoto et al., 2004). AAA proteins are widely distributed among eukaryotes, and are involved in a multitude of cellular functions, including regulation of the cell cycle, vesicle-mediated transport, peroxisome assembly, protein degradation by 26S proteasomes and transcriptional activation (Rechsteiner et al., 1993; Confalonieri and Duguetm, 1995; Lupas and Martin, 2002). Their functions are currently considered to be mediated through protein-protein interactions, in which structural change of AAA proteins after ATP hydrolysis appears to be critical (Botos et al., 2004). The molecular size greatly varies depending on the protein nature, but all possess the AAA domain, consisting of approximately 230 amino acid residues with Walker A and Walker B motifs and a distinguished conserved sequence, SRH (Lupas and Martin, 2002). Outside the conserved 230 amino acid module, the AAA proteins greatly differ among families, and no significant similarity can be detected in the N-terminal region. Walker motif A is specific for ATP binding and hydrolysis (Lupas and Martin, 2002).

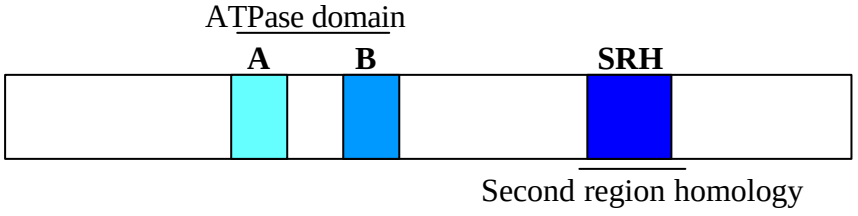

Figure 1. Structure of AAA protein100

Although more than 60 genes encoding the AAA conserved region have been registered from Arabidopsis, examples which have been functionally analyzed are few. Those include 26S proteasome (Fu et al., 1999), metalloprotease FtsH (Lindahl et al., 1996; Seo et al., 2000), NSF acting in vesicle trafficking (Rancour et al., 2002), PEX6 involved in peroxisome biogenesis (Olsen, 1998), Endoplasmic Reticulum-Golgi Network (Jou et al., 2006). NtAAA1 appears to be one of the first cases with involvement in pathogen responses, and we have proposed that it functions to alleviate detrimental excess HR during pathogen infection (Sugimoto et al., 2004). However, its molecular mechanisms have hitherto remained undetermined.

ARF proteins and stress responses

ADP-ribosylation factor (ARF) is a member of small GTPase, which is grouped into several major subfamilies including Ras, Rab, Rho, Ran, Arf and others (Zerial and Huber, 1995). Like other small GTPase, ARF contains GTP/GDP exchange regions, which are critical in GTP-induced conformational change and GTP hydrolysis (Bourne et al., 1991). It also has N-terminal myristoylation consensus sequence MGXXXS/AT at position 2 (Orci and Palmer, 1993). Mutation of glutamine amino acid residue at position 71 into leucine (Q71L) results in formation of active GTP-bound form, whereas replacement of threonine residue at position 31 with asparagine (T31N) resulted in inactive GDP-bound form (Dascher and Balch,

1994). ARFs have been known to cycle between active, membrane-bound form when associated with GTP, and an inactive, predominantly cytosolic form when bound to GDP. Inactive GDP-bound form interacts with guanine nucleotide exchange factors (GEFs) and GTPase-activating proteins (GAPs). In addition, active GTP-bound form bound to effector proteins mediates physiological functions of ARF. Active GTP-bound form interacts with a diverse group of proteins, including vesicle coat proteins and lipid-metabolizing enzymes (Nie et al., 2003).

ARF was originally identified in mammalian cells as a protein required for ADP-ribosylation of a subunit of heterotrimeric G protein Gs, thereby leading to activation of adenylate cyclase (Moss and Vaughan, 1995). Subsequent intensive studies have indicated that the principal role of ARF proteins is to regulate multiple steps in intracellular membrane traffic (Zerial and Huber, 1995). ARF proteins also directly interact with other proteins, including phospholipase D (Hammond et al., 1995; Jones et al., 1999), PIP2 (Liscovitch et al., 1994), arfaptin (Kanoh et al., 1997) and G protein subunit, Gs (Kahn and Gilman, 1986). In plants, ARF proteins have been reported to play certain roles in mitosis and in controlling the cell cycle during seed development (McElver et al., 2000), as well as in intracellular transport (Ritzenthaler et al., 2002). Rice ARF was suggested to be involved in disease response, as shown by analyses of transgenic tobacco plants which exhibited fungal pathogen resistance and rapid increase of pathogen-responsive gene expression (Lee et al., 2003). Despite these

observations, functions of plant ARF proteins remain largely unknown.

The aim and organization of this study

NtAAA1 appears to be one of the first cases with involvement in pathogen responses, and it functions to alleviate detrimental excess HR during pathogen infection (Sugimoto et al., 2004). However, little is known about its role and the molecular mechanisms, leading me to conduct following experiments with the aim to understand role of NtAAA1 and how it is regulated in response to pathogens.

(1) Analysis of *NtAAA1*-RNAi plants

(2) Differential micro-array screening to identify genes that were regulated by NtAAA1

(3) Isolation of NtAAA1 interacting protein, NtARF, by yeast two-hybrid screening

(4) Analysis of *NtARF* overexpressing transgenic plants

(5) Influence of NtAAA1 on NtARF-activated resistance

Chapter I

Suppression of salicylic acid signaling pathways by NtAAA1

Introduction

During the search for pathogen-responsive genes in tobacco plants, we identified an ATPase associated with a various cellular activities (AAA) protein (NtAAA1). NtAAA1 does not structurally belong to any of these classical AAA protein families, and is the first case of AAA protein that is involved in pathogen response.

In this chapter I, I describe that *NtAAA1*-RNAi transgenic plants exhibit an elevated resistance to *Pseudomonas syringae* infection. This suggested that *NtAAA1* negatively controlled the defense reaction, and subsequent screening identified involved genes. Results indicated NtAAA1 to act as a negative regulator of SA signaling pathway by mediating the JA signals.

Materials and Methods

Plant and bacterial materials

Wild type and RNAi transgenic tobacco plants (*Nicotiana tabacum* cv. Xanthi NC) were grown in a greenhouse at 23°C under a 14 h /10 h light/dark photocycle. Leaves from bout 2 month-old mature plants were detached and used for subsequent experiments. *Pseudomonas syringae* pv *glycinea* 801 was obtained from the Genebank of the Ministry of Agriculture, Forestry, Fisheries. Bacterial cells were grown in King's B medium at 25°C as described (King et al., 1954).

Pathogen and phytohormone treatments

P. syringae pv. *glycinea* 801 were grown to the density approximately 0.5 at 600 nm. Detached healthy leaves from wild type or *NtAAA1*-RNAi transgenic plants were subjected to bacterial injection using a syringe without needle, and incubated at 25°C for appropriate time periods up to 48 h. Leaf discs were collected immediately after infection (time 0), and periodically up to 48 h, homogenized in 10 mM $MgSO_4$, and crude extract was used as bacterial solution after appropriate dilution by plating onto KB agar. After incubation at 25°C for 1 day, number of colonies was visually determined. For treatments with phytohormones, healthy leaves were cut into 1.5-cm^2 pieces and placed in water for 4 h to diminish cutting stress. Resulting leaf pieces were submerged in a solution containing 0.5 mM salicylic acid dissolved in 0.05 % Triton X-100, or exposed to 50 μM jasmonic acid methyl ester in a sealed box. Samples were harvested at indicated time periods and used for further assay.

Detection of hydrogen peroxide and cell death

Cell viability was estimated by staining with an alcoholic lactophenol Trypan Blue mixture (30 ml ethanol, 10 g phenol, 10 ml water, 10 ml glycerol, 10 ml of 10.8 M lactic acid, and 10 mg of Trypan Blue). Samples were placed in a boiling water bath for 3 min, left at room temperature for 1 h, then transferred to a chloral hydrate solution (2.5 g ml^{-1}), and boiled for 20 min for destaining. Hydrogen peroxide was visualized using 3,3'-diaminobenzidine as the substrate (Thordal-Christensen et al., 1997). Leaves were excised and floated on solution containing 1mg ml^{-1} DAB for 5 to 8 h at 25°C. The treatment was terminated by immersion of the leaves in boiling ethanol (95%) for 10 min. After cooling, leaves were retained in ethanol and photographed.

Micorarray analysis

Detached leaves from wild type and NtAAA1-RNAi lines (R15-3, R15-8 and R15-9) were treated *P. syringae* pv. *glycinea* 801, and incubated at 25°C for 9 h. Total RNA was isolated as described (Chomczynski and Sacchi, 1987), and mRNA was prepared from 100 µg total RNA using a Gen Elutie mRNA miniprep kit (Sigma, St Lois, MO). The probe cDNA was synthesized and labeled with a Label Star Array kit (Qiagen, Helden, Germany). Independent experiments was performed using two duplicate slides with reverse labeling. cDNA differentially labeled with cy3 or cy5 was dissolved in 60 µl of hybridization buffer

(Amersham Life Science) and 120 µl of formamide. The probe was denatured at 95°C for 2 min and incubated at room temperature for 10 min. Printing slide procedures were preformed as described (Katoh et al., 2003). The slide was then exposed to UV crosslinker (ultraviolet crosslinker, Amersham Life Science). Careful handing of slide surfaces before hybridization as well as thorough steps ensured a minimum of dust. Microarray hybridization was performed by an automated slide processor (Amersham Biosciences) and then scanned by FLA-8000 version 1.0 Fuji Film, Tokyo). For data analysis, spot intensities from scanned slides were quantified by using Array vision version 6.0 (Amersham Biosciences). Grids were predefined and manually adjusted to ensure optimal spot recognition, discarding spots with dust or locally high background. Spots were individually quantified by using array vision. Gene expression data were normalized, and induced and repressed genes in *NtAAA1*-RNAi plants were selected based on values greater than 1.5 times of the wild type control.

RNA blot analysis

A 20-µg aliquot of total RNA isolated as described (Chomczynski and Sacchi, 1987) was fractionated on a 1% formaldehyde gel and blotted onto a nylon membrane. After immobilization by UV irradiation, blots were hybridized with appropriate ^{32}P-labeled probes in a solution containing 1 mM EDTA, 0.5% SDS, 50 mM Tris-HCl pH 7.5, 1×Denhardt's solution, 3×SSC, 50% formamide and 10% dextran sulfate at 42°C for 16 h. The membrane

was washed with 0.5×SSC containing 0.1% SDS at 65°C, and used to expose BAS (Fuji Photo Film, Tokyo, Japan) or x-ray film (Eastman-Kodak, Rochester, NY). The probes were radioactively labeled using [α-^{32}P]dCTP using a *Bca*BEST™ labeling kit (Takara, Kyoto, Japan).

Results

NtAAA1-silenced transgenic tobacco plants

In a previous report, we suggested that NtAAA1 might be involved in modulation of the resistance activity against pathogen attack through reducing the HR (Sugimoto et al., 2004). To directly verify this idea, we inoculated a pathogenic bacterium, *P. syringae* pv. *glycinea*, into healthy leaves of wild type and *NtAAA1*-silenced transgenic plants expressing a specific RNAi and periodically examined the disease symptoms (Figure 2). Transcripts of *NtAAA1* were induced 9 h after infection in wild-type plants, but not in transgenic line R15, indicating the RNAi to successfully function (Figure 2A). When leaves from wild type plants were challenged with the pathogen, distinct lesions were formed 24 h after infection and consistently developed into severe necrosis 48 h later (Figure 2B). In contrast, visible lesions scarcely developed on leaves from the transgenic R15 plants even after 48 h (Figure 2B). When cell viability was monitored by staining with trypan blue 24 h after inoculation, dead

cells were more abundant in R15 plants than in wild-type plants (Figure 2C, upper panel). Concomitantly, the level of hydrogen peroxide was also higher in R15 than in the control (Figure 2C, lower panel). Numbers of propagated bacteria in each inoculated leaf greatly differed. In wild type leaves, bacterial number linearly increased up to 6.5 x 10^6 after 48 h, while in transgenic leaves, the increase was much slower reaching only 10^5, being 1/15 that of the control (Figure 2D). These results suggested that active resistance actually took place in R15 leaves, although visible lesions were less evident, this being often observed in the case of non-host hypersensitive response (HR) (van Wees and Glazebrook, 2003; Takeuchi et al., 2003). Hence we concluded that, the HR was accelerated in R15 plants, and that this acceleration was apparently due to suppression of *NtAAA1* (Figure 2A). Concomitantly, expression of marker genes for HR, *PR-1a* and acidic *PR-2*, was higher in R15 than in the control (Figure 3, second and third panels). Densitometric estimation showed that transcripts for *PR-1a* and acidic *PR-2* were 5-fold and 1.7-fold higher than the control at 24 h, respectively (data not shown). These results were consistent with our previous observation that suppression of *NtAAA1* accelerated expression of HR-related genes (Sugimoto et al., 2004), and convinced us to proceed to the micro-array analyses.

Identification of differentially expressed genes

The micro-array analysis was performed using cDNA probes prepared from healthy

leaves of wild type and transgenic (line R15) plants. Leaf samples were inoculated with *P. syringae* pv *glycinea*, and harvested 9 h later, when expression of *NtAAA1* was the highest in the wild type plants (Figure 2A). A total of 330 genes was found to be differentially expressed in RNAi transgenic plants; 91 genes were up-regulated and 239 were down-regulated. Among up-regulated 91 genes, 82 were assigned to encode proteins with known function; for example, 21 were involved in stress response and defense (23%), 11 in metabolism (12%), 7 in cell structure (8%), and 7 in protein distribution and storage (8%) (Figure 4A). Among 239 down-regulated genes, 76 encoded proteins of unknown function (31%). The remaining included 29 genes encoding proteins involved in metabolism (12%), 21 in transcription (9%), and 22 in stress and defense (9%) (Figure 4B). Notably, defense-related genes appeared to be one of the major gene groups affected by NtAAA1. Among such genes, 10 were found to possibly participate in hormonal response (Table 1). Four genes were involved in the salicylic acid pathway, including *NPR1* (NP_916283), *ARF* (AAD17207), *Sar 8.2b* (M97359) and a gene for SA binding catalase (AAA57551). All were up-regulated in the transgenic line. Three were related to jasmonic acid response, *PLD* being up-regulated, and *LOX* and *thionin* down-regulated. The remaining 3 were involved in ethylene response; *ACCO* was up-regulated and genes for chitinase and ethylene-inducible protein were down-regulated (Table 1). For confirmation of these micro-array results, 5 genes representing different expression patterns were subjected to RNA gel-blot analysis using RNA samples isolated

Table 1. Selection of genes responding to signaling molecules.

Clone ID	BLAST hit	Putative function[a]	Ratio[b]	p-value[c]
Salicylic acid				
L-095_g04	M97359	Sar8.2b protein	3.22	0.020215
I-105_b01	AAA57551	Salicylic acid binding catalase	1.81	0.001289
R-101_h08	AAD17207	ADP-ribosylation factor, ARF	1.64	0.043165
R-112_f03	NP_916283	Putative Regulatory protein NPR1	1.58	0.018590
Jamonic acid				
I-031_e03	AAN05433	Phospholipase D delta isoform 1a	1.81	0.093642
R-038_a11	AAP83135	Lipoxygenase	0.28	0.001932
I-088_E03	BAA95697	Thionin like protein	0.19	0.039900
Etylene				
R-057_C09	AB012857	ACC oxidase	1.59	0.001023
Chitinase III	Z11563	Acidic chitianse III	0.10	0.002717
L-077_h02	AAA91063	Ethylene-inducible protein	0.05	0.048167

[a]Putative functions are based on sequence homology to known or predicted genes. [b]Ratio of relative expression intensity in *NtAAA1*-RNAi plants to that in wild type control plants after infection with *P. syringae* pv *glycine*. [c]Estimated by the test of significance at $p<0.05$.

from pathogen-treated leaves (Figure 5). Transcripts for *NPR1* and *ACCO* accumulated to a higher level in the transgenic line than in the wild type control, while those for *thionin, LOX* and *GRP* showed almost no accumulation. Results were consistent with micro-array data, which were thus proven to be reliable for further analyses.

Modulation of SA signaling pathway

The above-described results suggested that NtAAA1 may play an important role in

modulation of SA and JA pathways. Since suppression of NtAAA1 appeared to result in acceleration of SA pathway and in suppression of JA and ethylene pathways, effects of exogenously applied SA, alone and in combination with JA on expression of marker genes were examined (Figure 6). Experimentally, healthy leaves from wild type or *NtAAA1*-RNAi transgenic plants were detached and treated with SA for up to 48 h, and accumulation of *PR-1a* transcripts were profiled by the RNA blot hybridization. Results showed that, although transcripts were equally induced in both transgenic and control plants, the amount was over 3-fold higher in the former than in the latter (Figure 6A). When JA was simultaneously applied with SA, *PR-1a* induction was suppressed in both plants, but to a less extent in the transgenic line in comparison with the control (Figure 6B). These results suggested that NtAAA1 can attenuate the effect of SA, and that such an attenuation might be activated by the JA pathway.

Discussion

This paper documents that transgenic *NtAAA1*-RNAi tobacco plants showed an elevated resistance to pathogenic bacterium, *P. syringae* pv *glyciena*, in comparison with the wild type counterparts, and that such a resistance might be mediated through acceleration of salicylic acid signaling pathways. *Pseudomonas syringae* is one of the major gram-negative plant

pathogenic bacteria, which induce hypersensitive cell death in non-host plants (Taguchi et al., 2003). Inducible defense responses in non-host plants comprise the synthesis and accumulation of antimicrobial reactive oxygen species, phytoalexins, and translation products from pathogenesis-related genes as well as the localized reinforcement of the plant cell wall and hypersensitive programmed cell death (Mysore and Ryu, 2004; Numberger and Brunner, 2002; Thordal-Christensen, 2003). Our present results are consistent with this view, and clearly indicate that observed resistance was attributable to hypersensitive cell death through accelerated HR. In previous studies, we reported that, upon pathogen infection, *NtAAA1*-RNAi plants exhibited visible necrotic lesions to the same extent as the wild type plants (Sugimoto et al., 2004), but actual resistance activity was not directly estimated. In the present study, the same plants showed less lesions and high resistance, being apparently contradictory to the previous report. This inconsistence may be due to different experimental conditions, such as initial numbers of inoculated bacteria, age of leaf samples, humidity and temperature of cultivation, and incubation period, all of which are critical factors for effective induction of HR. A high level of resistance without clear lesion formation as observed here has occasionally been observed in non-host HR (van Wees and Glazebrook, 2003; Takeuchi et al., 2003). This is perhaps due to quick programmed cell death occurring at limited cells, thereby preventing the spread of visible tissue death as observed in ordinary HR.

Intensive survey has suggested that SA- and JA-signaling pathways are antagonistic

(Doares et al., 1995; Felton et al., 1999; Niki et al., 1998). For example, application of SA to tobacco leaves suppressed expression of genes encoding lipoxygenase-2, an enzyme for JA biosynthetic (Spoel et al., 2003) and thionin, an anti-fungal basic PR protein which typically responds to JA (Niki et al., 1998). The opposite is also true, as JA suppressed expression of genes for acidic PR proteins (Niki et al., 1998). However, the molecular mechanism of such antagonistic actions has not been established. It is generally considered that SA interferes with JA synthesis, and vice versa, resulting in shut-down of signaling pathway of the counterpart (Spoel et al., 2003; Laudert and Weiler, 2002; Doherty et al., 1988). Another idea is that whether SA or JA predominates depends on the concentration of each *in planta* (Mur et al., 2006). The present finding proposes an additional idea that, responding to JA signals, NtAAA1 directly suppresses SA signals.

The underlying mechanism is currently not clear, but two features must be separately considered; transcriptional level and protein interaction level. Since AAA proteins are supposed to be functional upon interaction with other proteins (Lupas and Martin, 2002), suppression of SA signals by NtAAA1 might be mediated through protein-protein interaction. In this context, it is conceivable that NtAAA1 is first activated by a JA-induced protein, and then interacts with SA-related protein(s), which in turn switch off the SA signaling. If it is the case, NtAAA1 might serve as a stand-by receptor of the JA signal. This is consistent with our previous observation that *NtAAA1* transcripts were evidently induced only by ethylene but not

by SA or JA (Sugimoto et al., 2004), indicating production of NtAAA1 itself to be independent on SA and JA. This hypothesis also accounts for the decreased expression of JA- and ethylene-responsive genes in *NtAAA1*-RNAi plants upon infection, as uncontrolled excess SA signals resulting in suppression and/or imbalance of JA/ethylene signaling pathways. Overall, it is tempting to speculate that NtAAA1 functions as a kind of molecular switch to shut down SA pathways.

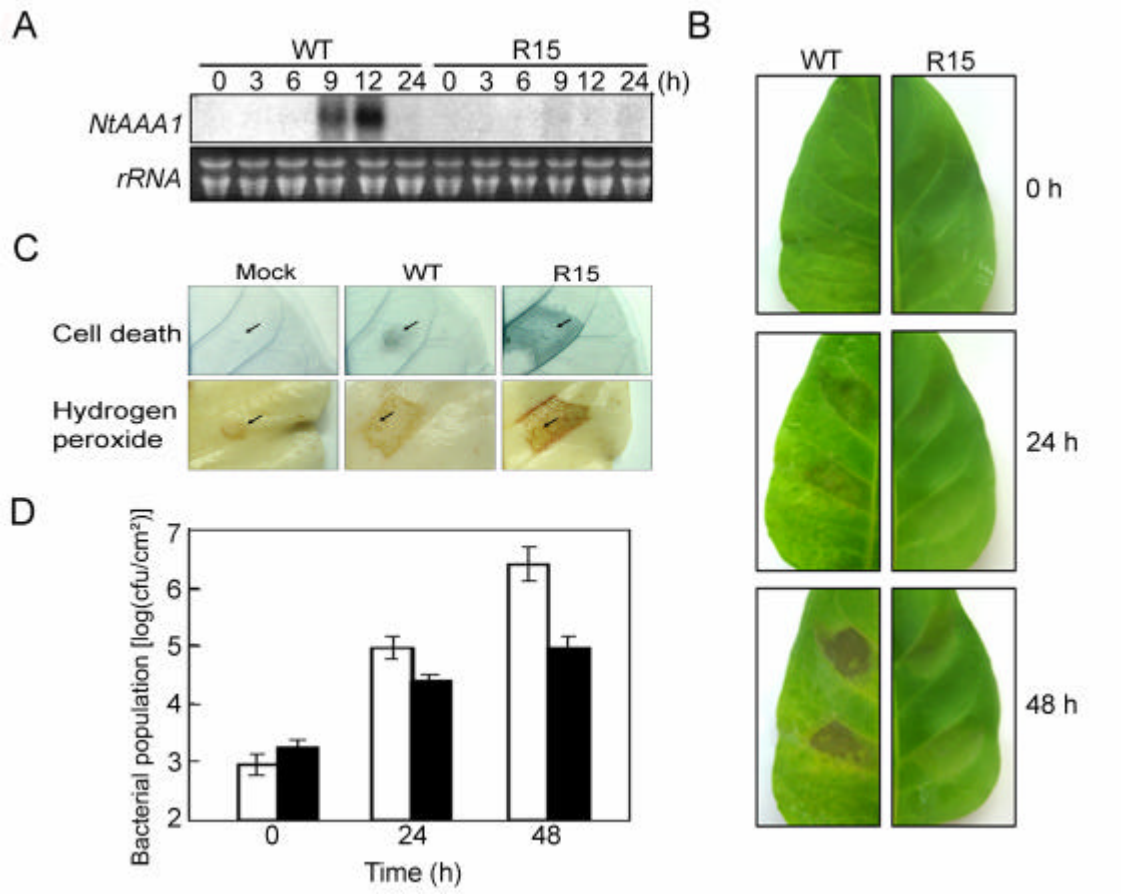

Figure 2. Properties of *NtAAA1*-RNAi transgenic tobacco plants.

(A) Confirmation of RNAi. Healthy leaves from wild type (WT) or transgenic line R15 (R15) were inoculated with *P. syringae* pv *glycinea* and incubated for indicated time period, when total RNA was extracted and subjected to RNA blot hybridization with *NtAAA1* cDNA as the probe. (B) Disease symptoms. Necrotic lesion development was observed at indicated time period after infiltration of *P. syringae* pv *glycine* into leaves from wild-type (WT) or RNAi transgenic line R15 (R15) plants. (C) Cell death and hydrogen peroxide production. After leaf samples from wild type (WT) or transgenic R15 (R15) were inoculated with *P. syringae* pv. *glycine*, cell viability was examined by trypan blue staining (upper panel), and hydrogen peroxide production was determined by 3,3'-diaminobenzidine staining (lower panel) 24 h after inoculation. Arrows indicate the position of infiltration of chemicals. (D) Quantification of *P. syringae* pv *glycine* cells propagated in wild type (open bar) or RNAi transgenic line R15 (R15) plants (closed bar). Leaf discs were collected at indicated time point after infection. Values are from triplicate measurements with standard deviation and expressed in logarithmic scale.

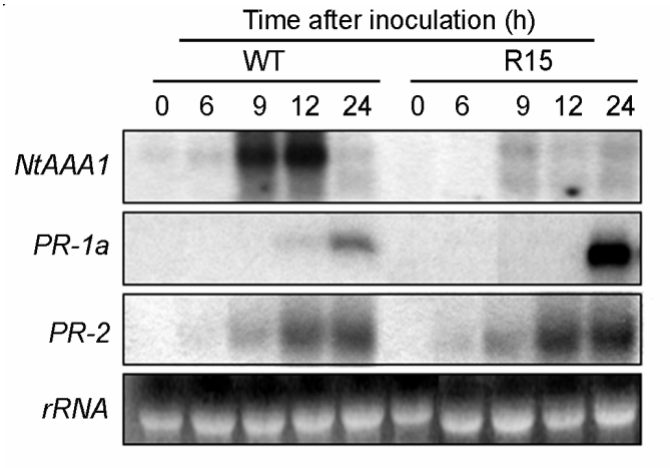

Figure 3. Accumulation profile of transcripts for defense related genes after inoculation of *P. syringae* pv *glycinea*.

Detached healthy leaves of wild-type (WT) and RNAi transgenic line (R15) were inoculated with *P. syringae* pv *glycinea* and incubated for indicated time period, when total RNA was extracted and subjected to RNA blot hybridization with probes for *NtAAA1*, *PR-1a* (X06361) and acidic *PR-2* (M5944). As the equal loading control, rRNA was used.

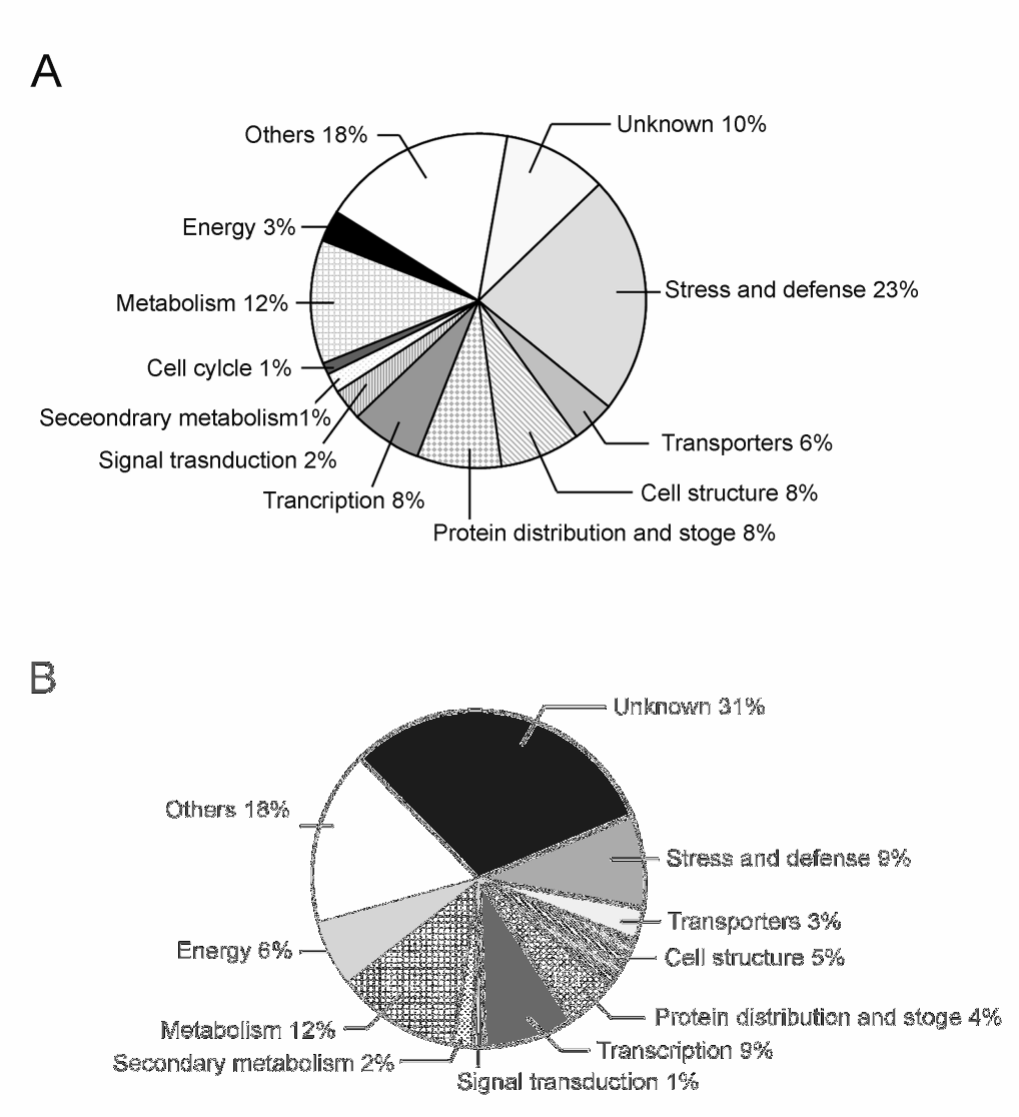

Figure 4. Identification of differentially expressed genes.

Healthy leaves from wild type or transgenic *NtAAA1*-RNAi line R15 plants were inoculated with *P. syringae* pv *glycinea* and incubated for 9 h. Total RNA was extracted and reverse-transcribed to yield probe cDNAs for microarray hybridization. Functional classification of 91 up-regulated (A) and 239 down-regulated (B) genes in the transgenic line in comparison with the control is shown with the ratio to the total gene numbers in percentage.

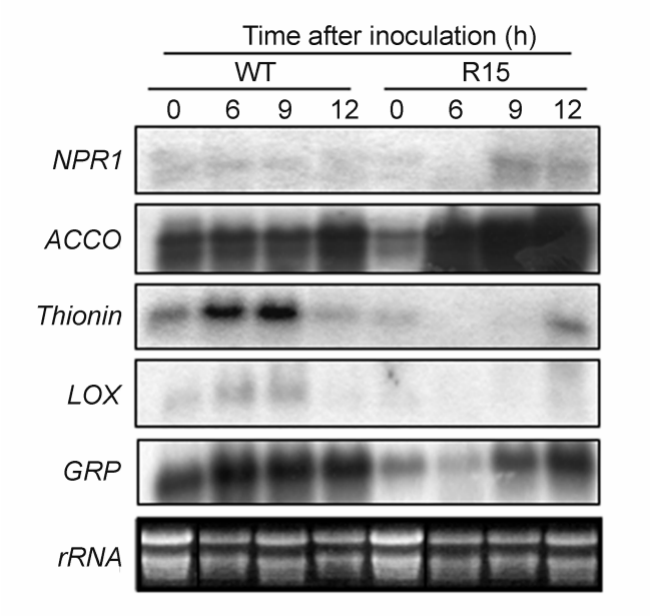

Figure 5. RNA blot hybridization.

Healthy leaves from wild type (WT) or transgenic *NtAAA1*-RNAi line R15 (R15) plants were inoculated with *P. syringae* pv. *glycinea*, incubated for indicated time period and total RNA was extracted, which was fractionated on agarose gel and blotted onto nylon membrane. Hybridization was performed with indicated probe cDNAs prepared after microarray results. Probes were, *NPR1* (nonexpresser of PR gene 1, NP_916283), *ACCO* (aminocyclopropane carboxylic acid oxidase, AB012857), *Thionin* (BAA95697), *LOX* (lipoxygenase, AAP83135), *GRP* (glycine rich protein, M37152). As the equal loading control, rRNA was used.

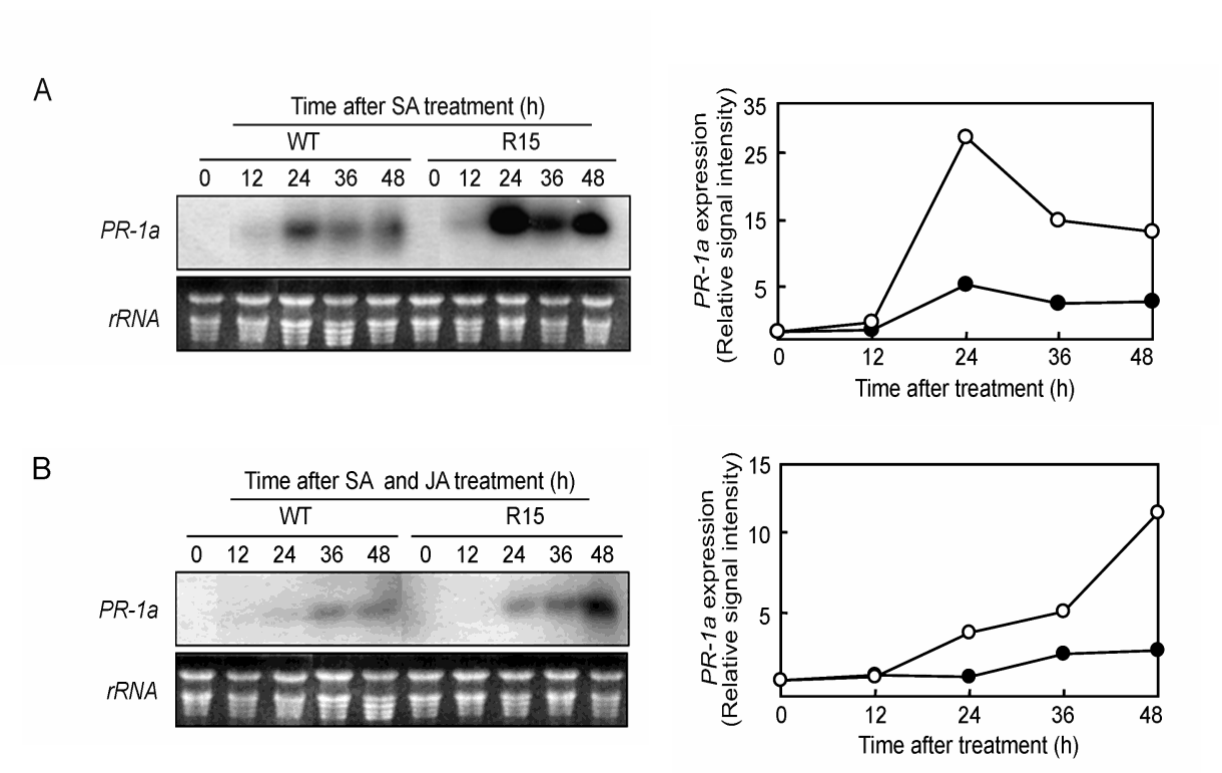

Figure 6. Effects of exogenously applied signaling molecules.

Leaves of wild type (WT) and transgenic *NtAAA1*-RNAi (R15) plants were cut into 1.5-cm^2 and floated on buffer solution containing 500 µM SA (A), or 500 µM SA and 50 µM JA methyl ester (B) and sampled at indicated time periods. Total RNA was isolated and subjected to RNA blot hybridization with the *PR-1a* probe (left panel). Signals are densitometrically quantified (right panel). As the equal loading control, rRNA was used.

Chapter II

Attenuation of the hypersensitive response by NtAAA1 through suppression of a small GTPase, ADP ribosylation factor in tobacco plants

Introduction

In chapter I, I analyzed transgenic tobacco plants expressing the *NtAAA1*-RNAi, and suggested that NtAAA1 acts as a negative regulator of the SA signaling pathway by mediating the JA signals, thereby serving as a molecular switch for SA signaling pathways. However, the molecular mechanism of NtAAA1 is still unknown, and attempted molecular characterization of NtAAA1 in this chapter. To this end, I used a yeast two-hybrid system to screen for proteins that interact with NtAAA1. I first describe isolation of NtAAA1 interacting protein, a small GTPase, NtARF. Then, I report that *NtARF* overexpressing transgenic plants exhibited spontaneous and wound-induced lesion formation and enhanced resistance to pathogen attack. Finally, I investigated that expression of *NtAAA1* in leaves of NtARF transgenic plants attenuated lesion formation and suppressed pathogen resistance, and that the molecular basis for the known antagonistic actions of ethylene and salicylic acid in defense response could be partly attributable to these two proteins.

Materials and Methods

Plant materials and phytohormone treatment

Wild type and transgenic tobacco plants (*Nicotiana tabacum*, cv. Xanthi nc) were grown in a greenhouse at 23°C under a 14 h/10 h light/dark photocycle. About 2 month-old mature leaves were detached and used for subsequent experiments. For exposure to phytohormones, detached leaves were placed in water for 4 h to diminish cutting stress, and treated with 2 mM salicylic acid (SA) dissolved in 0.05 % Triton X-100, 50 μM jasmonic acid methyl ester (MeJA) or 100 μM ethephon to produce ethylene in sealed boxes.

Pathogen infection and agroinfiltration

Pseudomonas syringae pv. *glycinea* 801 (a generous gift of Y. Takagaki) was grown in King's B (KB) medium at 25°C. Wild-type and transgenic plants were grown in a greenhouse for 4 weeks. Healthy leaves were then detached and treated with *P. syringae* pv. *glycinea* 801 (absorbancy at 600 nm was approximately 0.5) by injection using a syringe without a needle and incubated at 23°C for an appropriate time period up to 3 days. Bacterial growth was estimated by counting bacterial numbers in leaf discs, which were collected immediately after infection (time 0), and periodically up to 3 days, and homogenized in 10 mM $MgSO_4$ solution. After appropriate dilution, bacteria were plated onto KB agar, on which *Agrobacterium* can

not grow, incubated at 25°C for 1 day, and numbers of colonies were counted. Agroinfiltration was performed as described (Ueda et al., 2006). Briefly, a 100 µl solution containing *Agrobacterium tumefaciens* strain LBA4404 with or without transgene expression vector was infiltrated into intercellular spaces of fresh leaves, which were maintained in a growth cabinet at 23°C under a 14 h/10 h light/dark photocycle.

RNA isolation, northern hybridization and RT-PCR

A 20-µg aliquot of total RNA isolated as described (Chomczynski and Sacchi, 1987) was fractionated on a 1% formaldehyde gel and blotted onto a nylon membrane. After immobilization by UV irradiation, blots were hybridized with appropriate ^{32}P-labeled probes in a solution containing 1 mM EDTA, 0.5% SDS, 50 mM Tris-HCl pH 7.5, 1×Denhardt's solution, 3×SSC, 50% formamide and 10% dextran sulfate at 42°C for 16 h. The membrane was washed with 0.5×SSC containing 0.1% SDS at 65°C, and used to expose BAS (Fuji Photo Film, Tokyo, Japan) or X-ray film (Eastman-Kodak, Rochester, NY). The probes were radioactively labeled using [α^{32}P]dCTP using a *Bca*BEST^{TM} labeling kit (Takara, Kyoto, Japan). RT-PCR were performed using SuperScript II, 1µg of total RNAs from each sample and the oligo(dT)$_{12-18}$ primer under the conditions described by the manufacturer (Invitrogen). First-strand cDNA synthesized was amplified with different sets of specific primers to estimate the transcripts level of *NtAAA1* and *rRNA*.

Yeast two-hybrid screening

The MATCHMAKER yeast two-hybrid system (Clontech, Palo Alto, CA) was employed to screen for proteins interacting with NtAAA1. A tobacco cDNA library was prepared as fusion products in vector pGADT7 (Clontech) using mRNA from leaves and transformed into a yeast strain, AH109. Full length *NtAAA* was cloned into a bait vector (pGBKT7) to produce a fusion protein and transformed into the yeast strain, Y197. Cell growth was examined on SD agar plates containing appropriate amino acids without trytophane, leucine, histidine and adenine hemisulfate salt. Quantification of binding activity was estimated by β-galactosidase assay according to the manufacturer's instructions (Clonetech).

Epifluorescence analysis

Full length NtARF1 cDNA prepared by PCR was inserted into *Sal*I and *Nco*I sites of pGEM T-easy vector (Promega, Madison, MI), propagated and insert fragments were ligated into appropriate sites of sGFP (s65T) vector. The GFP-NtAAA1 was prepared as described (Sugimoto et al., 2004). For co-localization experiments, *NtARF* and *NtAAA1* sequences were amplified using appropriate primers. Primers for *NtARF* were: forward, 5'-TATGGGGCTGTCTTTCGGCAAAC-3'; *xba*I-reverse, 5'-GCTCTAGAGCCTATGCCTTGTTTGAAATATTGTT-3'. Primers for *NtAAA1* were: *Bgl*II-forward, 5'-AGATCTATGAGCACAATGGGATTGCT-3', *xba*I-reverse,

5’-TCTAGAATTTTGGGTAAAACCATCTAAACT-3’. After digestion with *Bgl*II and *xba*I, the construct was introduced into a CFP vector. PCR product of *NtAAA1* was inserted into *Bgl*II and *xbal*I sites of pGEM T-easy vector (Promega, Madison, MI), propagated and inserted fragments were ligated into appropriate sites of the YFP vector. Gold particles coated with resulting plasmids were bombarded into onion epidermal cells according to the manufacturer’s instructions (PDS-1000, Bio-Rad Laboratories, Hercules, CA) at a pressure of 1100 psi. Intracellular fluorescence analysis was performed by a confocal laser scanning microscope using a Zeiss LSM 510 microscopy system (Carl-Zeiss) with an Argon ion laser as an excitation source after incubation in the dark at 25^{o}C for 12 h. Fluorescence of CFP- and YFP-tagged proteins, expressed in onion epidermal cells was observed under a microscopy equipped with appropriate filters.

Fluorescence resonance energy transfer assay

FRET-experiments were performed by confocal laser scanning microscope using a Zeiss LSM 510 Meta (Carl-Zeiss) operating with argon laser. The laser was tuned to lines at 458 and 514 nm. CFP- and YFP-tagged proteins were excited by the 458 nm and the 514 nm laser lines sequentially. The FRET signal was detected by YFP fluorescence in the range at 458 nm excitation. Cell were bleached in the acceptor YFP channel by scanning a region of interest (ROI) around the cytoplasm and plasma membrane using 100 times 514 nm argon laser line at

100 % intensity. The bleach time ranged from 10 sec. Before and after the acceptor bleaching, the CFP intensity images were collected to assess the changes in the donor fluorescence. FRET efficiency was calculated using the following formular : $(I_5\text{-}I_4) \times 100/ I_5$, where I_5 is the CFP intensity after the photobleaching of YFP and I_4 is the intensity just before the photobleaching.

Construction of mutated ARF

Point mutations were introduced into *NtARF* by PCR site-directed mutagenesis. Q71L and T31N substitutions were achieved using the two-step recombinant PCR technique, by which two fragments having overlapping regions at 3' and 5'-ends were initially generated. Primers for the Q71L mutation were: for the 5'-fragment; 5'-TATGGGGCTGTCTTTCGGCAAAC-3' (forward), and 5'-TAGTGGTCGAATCTTGTCTAGACC-3' (reverse); and for the 3'-fragment; 5'-CTTGTAGAGAATTGTGTTTTTACC-3' (forward), and 5'-GGTCTAGACAAGATTCGACCAC-3' (reverse). Similarly, primers for the T31N mutation were: 5'-CTTGATGCTGCTGGTAAAAACACAA-3' (forward), and 5'-TGCCTTGTTTGAAATATT-3' (reverse), with the introduced point mutation underlined. Amplified pairs of overlapping fragments were then combined with the forward and reverse primer to generate full-length mutants by second PCR. Resulting cDNAs for point mutated

NtARF (*NtARF*^{Q71L}, *NtARF*^{T31N}) and also wild type *NtARF* were isolated by blunt-end polymerase chain reaction (PCR) and inserted into appropriate sites of the pBAD102/D-TOPO vector (Invitrogen) for further cloning.

Pull-down assays

Glutathione-*S*-transferase-NtAAA1 fusion proteins were produced in *E. coli* BL21 by incubation at 18^{o}C for 12 h in the presence of 1 mM isopropyl β-D-thiogalactopyranoside (IPTG) (Sugimoto et al., 2004). Solubilized proteins generated by sonication were purified through glutathione-Sepharose 4B beads following the manufacturer's instructions (Amersham, Uppsala, Sweden). His-tagged NtARF, NtARF^{Q71L} and NtARF^{T31N} proteins were produced in *E. coli* (BL21) cultured at 37^{o}C for 4 h after adding arabinose at a final concentration of 0.2%. The resulting fusion proteins were purified using Ni-NTA beads following the manufacturer's instructions (Qiagen) and amounts were measured by the Bradford method (1976). GST-NtAAA fusion protein (5 μg) was incubated with glutathione-agarose beads (50 μl of 50% beads) in 200 μl binding buffer for 2 h at 4^{o}C with gentle shaking. The beads were collected by brief centrifugation, washed twice with 500 μl washing buffer, incubated with blocking buffer (5% skimmed milk, DTT) at 4^{o}C for 1 h, and then washed with 500 μl washing buffer. They were then incubated with 25 μg of NtARF, NtARF^{Q71L} or NtARF^{T31N} proteins in 200 μl binding buffer at 4^{o}C for 2 h, and washed three

times with washing buffer containing 0.5% Tween 20. NtAAA on the beads was eluted with GST elution buffer, suspended in 100 µl, and after fractionation on 10% SDS-PAGE, subjected to western blot analysis using anti-His antibodies. For GTP analog testing, 25 µg of NtARF-His fusion protein was incubated with 1 mM GTP[γS] or GDP[βS] in binding buffer containing 5mM $MgCl_2$ at 30°C for 40 min prior to incubation with GST-NtAAA (5 µg) bound beads. Similarly, for ATP analog testing, 25 µg of GST-NtAAA was incubated with 1 mM ATP[γS] or ADP[βS] in binding buffer containing 5 mM $MgCl_2$ at 30°C for 40 min prior to addition of NtARF and its mutants.

Plant transformation

Transgenic tobacco plants (*N. tabacum* cv. Xanthi nc) were produced as previously described (Yap et al., 2002). Briefly, full length *NtARF* cDNA was ligated into the *BamH*I and *Xba*I sites of a plant binary vector *pBI121* (Clontech), which was introduced into *A. tumefaciens* strain LBA4404 cells.

Results

Identification of NtARF

Since AAA proteins are considered to function through protein-protein interactions

(Birschean et al., 2005; Vale, 2000), we decided to identify proteins directly interacting with NtAAA1 by yeast two-hybrid screening using a tobacco cDNA library with NtAAA1 as the bait. Among 6 clones initially screened, one particular clone was finally obtained (Figure 7A), and sequence analysis revealed this clone shared a high identity with a small GTPase, ARF GTPases (Figure 7B). Accordingly it was designated as *NtARF* (*Nicotiana tabacum* ARF) (accession no. AB2743060). We conducted a phylogenetic analysis of NtARF from ARF GTPase and other a small GTPase such as RAN, ROP and RAB GTPase. ARF GTPase appear separated from other GTPase and distributed into four groups, ARF, ARL II and SAR, AFL I. NtARF belongs to the ARF subgroup, which share 98% identity with AtARFA1e and OsARF1 (Figure 8). Their physiological functions are considered to be involved in vesicle budding in different steps of membrane trafficking (Vernoud et al., 2003). Accumulation profiles of *NtAAA1* and *NtARF* transcripts were examined by RNA blot analysis with total RNAs isolated from leaves inoculated with *P. syringae* pv. *glycinea*. Hybridization with cDNA probes for each gene revealed that, transcripts for *NtAAA1* and *NtARF* were clearly induced 9 h and 3 h after infection, respectively (Figure 9). The results suggested that the two genes are differentially expressed upon pathogen infection, and that protein-protein interactions might selectively occur when NtAAA1 is produced in the late stages of infection.

Mode of interaction

Interaction between NtAAA1 and NtARF was confirmed by in vitro pull-down assay. Bacterially expressed His-tagged NtARF was applied to a glutathione-Sepharose column containing GST-tagged NtAAA1 or GST proteins, eluted with a buffer containing reduced GST, separated by SDS-PAGE and subjected to immuno-blot assays with anti-His-tag antibodies. The results clearly showed His-tagged NtARF to be detectable upon incubation with GST-tagged NtAAA1 but not with GST protein alone, indicating specific binding of NtARF to NtAAA1 (Figure 10A, lane 3). Activity of small GTPases including ARF is reversibly regulated by GTP and GDP (Nie et al., 2003), with activation on binding to GTP and inactivation by the hydrolysis of GTP to GDP. To determine whether such conversion of NtARF might influence its interaction with NtAAA1, mutated NtARF was constructed and subjected to binding assays. An active ($NtARF^{Q71L}$) form was prepared by substituting glutamine at the position 71 into leucine (Q71L) and an inactive form ($NtARF^{T31N}$) was made by replacing threonine at position 31 with asparagine (T31N) (Dascher and Balch, 1994). *In vitro* pull-down experiments showed that NtAAA1 efficiently bound NtARF when it was in the active form ($NtARF^{Q71L}$), but not at all in the inactive from ($NtARF^{T31N}$) (Figure 10A, lanes 4 and 5). This specificity was further confirmed by binding assay in the presence of GTP analogs, GTP[γS] and GDP[βS], neither of which are metabolized, resulting in constitutive formation of active and inactive NtARF, respectively. Pull-down results again showed preferential binding of NtAAA1 to the active form of NtARF (Figure 10B).

Activity of AAA proteins is also considered to be reversibly regulated by ATP and ADP (Jou et al., 2006), in this case due to a change in their conformation due to the energy of ATP hydrolysis, with acquisition of the ability to interact with partners (Vale, 2000). Interactions between NtAAA1 and NtARF were therefore examined in the presence of ATP[γS] or ADP[βS], both of which are able to bind to NtAAA1 but not are turned over, forming active or inactive protein complexes, respectively (Figure 10C). GST-tagged NtAAA1 was pre-incubated with either ATP[γS] or ADP[βS], and then tested for binding to NtARF, using either active ($NtARF^{Q71L}$) or inactive ($NtARF^{T31N}$) forms. The results showed two features; first, NtAAA1 only bound to the active form of NtARF, and second, such binding appeared to be stronger in the presence of ATP[γS] than with ADP[βS] (Figure 10C). Indeed, densitometric estimation pointed to a 2.1-fold higher signal intensity for the former (data not shown). Overall, these observations suggested that the interaction favorably takes place when both proteins are in active forms, i.e., NtAAA1 in ATP-bound and NtARF in GTP-bound forms.

Co-localization

Intracellular localization of NtARF and NtAAA1 was first examined using GFP-fusion proteins, driven by the cauliflower mosaic virus (CaMV) 35*S* promoter. Transient expression by particle bombardment into onion epidermal cell layers showed fluorescence from the

control 35S-GFP to be observed throughout cells (Figure 11A). Fluorescence from oth NtAAA1-GFP and NtARF-GFP was mainly observed in cytoplasmic and membrane fractions (Figure 11A). When NtAAA1 was fused to yellow fluorescent protein (YFP) and NtARF to cyan fluorescent protein (CFP), and simultaneously expressed in a single cell, both clearly overlapped at inside the cytoplasm and plasma membrane (Figure 11B), strongly suggesting their interaction *in vivo*. Interactions between NtAAA1 and NtARF in planta were directly analyzed by the fluorescence resonance energy transfer (FRET) assay, in which YFP and CFT fusion proteins were simultaneously expressed in cells and examined as donor-acceptor pairs. Onion epidermal cells transiently expressing YFP-NtAAA1 and CFP-NtARF were microscopically observed before and after bleaching (Figure 12A). With the bleaching of YFP-NtAAA1 fluorescence, a sharp and sudden increase in the intensity of CFP-NtARF was observed (Figure 12A, 4). The energy transfer was then quantified at the region of interest (ROI) as marked by circles (Figure 12A). Results showed as much as 64.9% increase of CFP fluorescence (Figure 12B, upper panel), indicating that a typical protein-protein interaction took place *in vivo*. Control cells expressing CFP did not show any increase in fluorescence intensity after the bleaching of YFP (Figure 12B, lower panel).

NtARF overexpressing transgenic tobacco plants

Functions of NtARF and its relationship to NtAAA1 were further examined using

transgenic tobacco plants constitutively expressing *NtARF* under the control of the CaMV35*S* promoter. Among 15 transgenic lines initially produced, 5 were finally selected and overexpression of the introduced gene was confirmed by RNA blot hybridization (Figure 13A, upper panel). Phenotypically, these transgenic plants often exhibited spontaneous necrotic spots on mature leaves (Figure 13A, two representative lines shown at lower panel), and one line (S5) was selected as the representative for further analysis. During the growth, such lesions were found to be absent on young leaves. Since untransformed wild-type plants grown under the same condition did not show any lesions at the same leaf positions, they appeared due to expression of the introduced *NtARF* gene, as this was found at equal levels in all transgenic leaves regardless of the age (Figure 13B, upper panel). Since the more senescent the leaves, the more the accumulated stress, this might explain greater sensitivity to stimuli for necrotic cell death. This idea is supported by the finding that a necrosis marker gene, *PR-1a*, was highly expressed in damaged, but not in apparently undamaged leaves (Figure 13B, lower panel). It is notable that expression of *NtAAA1* was not linked to that of *NtARF*, even in leaves showing severe lesions (Figure 13B, lower panel). Concluding that transgenic leaves are in a hypersensitive state even under non-stressed conditions, we assessed their response to pathogen infection. When wild-type leaves were inoculated with *P. syringae* pv. *glycinea*, disease symptoms were visible 24 h later, and tissue death was evident after 48 h (Figure 13C). In contrast, disease symptoms were scarcely observed in inoculated transgenic

leaves at 24 h, and tissue death was still unclear even after 48 h (Figure 13C). Concomitantly, bacterial growth in transgenic leaves was retarded to 1/10 that in the wild-type (Figure 13D, values expressed in log scale). It was concluded that NtARF plays a positive role in defense responses against pathogen attack, perhaps by accelerating the HR.

Antagonistic action of NtAAA1 against NtARF

The influence of NtAAA1 on NtARF-activated hypersensitivity was finally examined. Since mechanical injury triggered HR-like responses in transgenic plants overexpressing *NtARF* (data not shown), a simple experiment was set up, in which leaves were wounded by infiltration with *Agrobacterium* harboring either *NtAAA1* expression vector or a corresponding empty vector as the control. When *NtARF*-transgenic leaves were infiltrated with the control vector (mock), and incubated for 5 days, clear tissue death was observed (Figure 14, upper part of right panel). When the same leaves were infiltrated with the *NtAAA1* expressing vector, tissue death was hardly apparent (Figure 14, lower part of right panel). The same treatments of wild type leaves did not cause any lesions (Figure 14, left panel). These results indicated that NtAAA1 suppressed tissue death caused by NtARF upon wounding by mutual interaction *in planta.*

Effects on pathogen resistance were finally examined. Healthy leaves from each of three independent transgenic lines (S1, S2 and S5) were simultaneously infiltrated with *A.*

tumefaciens haboring the *NtAAA1* expression vector and *P. syringae* pv. *glycinea*, and lesion development was periodically examined (Figure 15). As the control, *A. tumefaciens* harboring the empty vector was used (mock). Expression of introduced *NtAAA1* was confirmed by RT-PCR, showing clear accumulation of its transcripts 72 h later in both wild type and S5 leaves (Figure 15B). In leaves from wild type controls, necrosis was distinct 2 days after infiltration, and further developed thereafter. Development of lesions was seemingly similar whether *NtAAA1* was expressed or not (Figure 15A, left panel). In contrast, mock-treated leaves from transgenic lines exhibit less necrosis at day-2, and slower lesion development at day-3 in comparison with the control (Figure 15A, three panels from right). When *NtAAA1* was expressed, the progression of lesion formation was accelerated, indicating suppression of resistance (Figure 15A, right panel). In order to quantify NtAAA1 effects, numbers of propagated *P. syringae* pv. *glycinea* in each inoculated leaf were then counted (Figure 15C). In mock-treated leaves of wild type, bacterial number linearly increased up to 5×10^6 after 48 h. When *NtAAA1* was expressed, the increase was even accelerated to 8.5×10^6, a 1.7-fold that of the control, indicating resistance being retarded. In contrast, bacterial number was only 5.2×10^5 in mock-treated transgenic leaves, being 1/10 of the wild type, consistent with previous observation (Figure 13D). When *NtAAA1* was expressed in transgenic leaves, bacterial number increased to 2.3×10^6, a 5-fold higher than that in the absence of *NtAAA1* expression. This value is comparable with the mock-treated wild type control, clearly

indicating the counteraction of NtAAA1 against NtARF (Figure 15C). It is notable that, in transgenic line S5, mechanically wounded areas by infiltration showed clear lesions upon mock-treatment, while almost none were visible with *NtAAA1* expression (Figure 15, right panel). It is clear from these observations that NtAAA1 indeed interferes with NtARF, which confers resistance against pathogen attack.

Transcript induction

Profiles of accumulated transcripts of *NtAAA1* and *NtARF* after treatment with signaling substances were examined. When healthy tobacco leaves were treated with salicylic acid (SA), *NtARF* transcripts were transiently induced 6 h later, with gradual decline thereafter up to 36 h, while *NtAAA1* transcripts were essentially lacking (Figure 16A). In contrast, when leaves were exposed to ethylene, the level of *NtARF* transcripts did not change, maintaining a low background level, while *NtAAA1* transcripts were markedly increased after 6 h later, with further gradual increment up to 72 h (Figure 16B). Jasmonic acid (JA) did not exhibit any effects on either gene (Figure 16C). Thus *NtARF* and *NtAAA1* were found to be differentially activated by SA and ethylene, respectively, and the antagonistic actions of ethylene and SA during pathogen responses (Wang et al., 2002) might partly be mediated through these two proteins.

Discussion

This paper documents strong evidence that plants are equipped with a system for suppressing excessive defense responses to wounding and pathogen attack. Physiologically it is well established that stress responses are well balanced, so that plants can best cope with changes in environmental conditions. For example, lesion development in TMV-infected leaves ceases at certain stages, with formation of clear ring-shaped necrotic tissues which confine pathogen particles and protect the surrounding areas (Waller et al., 2006). In the present study, we found that protein-protein interactions might be involved in the molecular mechanisms responsible for maintaining an equilibrium between promotion and depression of lesion formation.

ARF proteins and stress responses

NtAAA1 is a protein consisting of 497 amino acid residues with a molecular mass of 57 kDa. Phylogenetic analysis indicated that it is rather distantly related to classical AAA protein groups, making it difficult to speculate its functions based on sequence data alone (Sugumoto et al., 2004). However, since *NtAAA1* transcripts were specifically induced during the hypersensitive response (HR) upon infection with TMV and *P. syringae* pv *glycinea*, we constructed *NtAAA1*-RNAi transgenic tobacco plants, and examined their physiological and molecular features in detail. Results clearly indicated that NtAAA1 negatively regulates

defense reactions, possibly by interacting with specific protein(s), which positively function during the HR.

Subsequent screening identified an ARF protein, NtARF, for which overexpression indeed accelerated pathogen resistance. Arabidopsis contains 21 genes encoding ARF proteins, which are phylogenetically classified into four groups, SAR, ARF, ARF-like (ARL) I and ARL II (Vernoud et al., 2003). The SAR subgroup is necessary for coat protein complex II (COP II)-defendant transport from endoplasmic retriculum (ER) to Golgi, whereas the ARF subgroup regulates both COP I-dependent retrograde transport in the Golgi and clathrin-depedent budding from the trans Golgi and the PM. ARF subfamily also regulate lipid-metabolizing enzymes (Nie et al., 2003) and actin remodeling (Donaldson, 2000). ARLs are not as well characterized as SARs and ARFs, an ARL-knockout have been reported to play certain roles in mitosis and in controlling the cell cycle during seed development (McElver et al., 2000). NtARF could be assigned to the ARF group, as its amino acid sequence shares 98% identity with two proteins belonging to this group, AtARFA1e and OsARF1. Physiological functions of ARF proteins are not completely elucidated, but generally they are considered to be involved in vesicle formation and intracellular vesicle trafficking (Lee et al., 2002; Takeuchi et al., 2002; Sieburth et al., 2006; Song et al., 2006). The ARF subgroup appears involved in COP-I and clathrin-dependent budding from the trans-Golgi and plasma membrane (Vernoud et al., 2003). Recent studies suggested that they

also contribute to regulation of lipid-metabolizing enzymes (Nie et al., 2003) and actin remodeling (Donaldson, 2000). Wounding triggers activation of ARF GTPase, resulting in the activation of PLD activation and cytoskeleton remodeling cascade to lead wound closure (Turner and Brown, 2001). A notable aspect of plant ARF proteins is a clear involvement of OsARF1 in plant defense, enhancing disease resistance against pathogens with concomitant induction of salicylic acid (SA)-activated PR genes (Lee et al., 2003). Our present findings are consistent with the conclusion that NtARF triggers hypersensitive cell death and suggest more diverse function of ARF proteins in plants than hitherto speculated.

Interactions between NtAAA1 and NtARF

A unique finding of the present study is that an AAA protein interferes with ARF function by direct molecular interactions. However, this does not appear to be simple protein-protein binding, since both proteins are known to reversibly change their activity upon binding to nucleotides. ARF proteins are activated by GTP binding and inactivated by hydrolysis yielding the GDP-form (Bourne et al., 1991). AAA proteins are also activated by ATP-binding, using the energy of ATP hydrolysis, and inactivated in ADP-binding forms (Vale, 2000; Botos et al., 2004).

Mutual interactions between NtARF and NtAAA1 could theoretically involve four combinations; active NtARF and active NtAAA1, active NtARF and inactive NtAAA1,

inactive NtARF and active NtAAA1, and inactive NtARF and inactive NtAAA1. To determine which combination is most effective, we performed mutation and nucleotide analog analyses, and found the interaction to predominantly occur between the two active forms. This finding is important in considering the biological significance of NtARF-NtAAA1 interactions. It is thus conceivable that the defense response is initiated by activation of NtARF, but suppressed subsequently by its inactivation by activated NtAAA1, consistent with the observed physiological features. The question then arises as to how these two proteins are differentially controlled regarding temporal and spatial aspects of their activation.

Tuning of the hypersensitive response

Differential induction of transcripts of each gene upon pathogen attack is one clue. In the present study, transcripts for *NtARF* began to accumulate 3 h after infection, while those for *NtAAA1* were induced 9 h later and thereafter. Although transcriptional features do not necessarily directly reflect protein activity, these observations are consistent with a view that newly synthesized NtARF participates in the initial activation of defense response, and that NtAAA1 produced at later phases inactivates the former, resulting in a gradual decline of the defense response.

Another clue is their differential response to signaling molecules. SA treatment activates *NtARF* but not *NtAAA1*, while the opposite is the case with ethylene, and JA affects neither. It

is generally considered that SA positively mediates pathogen response by activating genes involved in defense reaction, while ethylene and JA are associated with wound responses (Felton and Korth, 2000). However, physiological and molecular analyses with various mutant lines have suggested rather complicated inter-relationships, with cooperative as well as antagonistic regulation (Doares et al., 1995; Felton et al., 1999). For example, SA-dependent and JA/ethylene-dependent pathways induce expression of different sets of *PR* genes, resulting in diverse resistance to different pathogens (Glazebrook, 1999; Wang et al., 2002). However, SA and JA/ethylene signaling pathways may also demonstrate mutual interference under certain circumstances (Jirage et al., 2001; Wang et al., 2002). The available data indicate that SA and JA/ethylene pathways interact both positively and negatively depending on pathogen types and specificity of defense response, although molecular bases for such interactions have yet to be clearly established (Wang et al., 2002). Our finding that SA-induced NtARF is suppressed by ethylene-induced NtAAA1 may well at least partially explain antagonistic regulation with SA and ethylene. SA/ethylene interference may take place not only at the level of signaling pathways, but also at the level of protein-protein interactions, thus enabling plants to modulate their HR quickly, finely and locally.

Overall, the present study clearly showed that plant defense is substantially regulated at the protein level. Since both ARF and AAA proteins have been suggested to participate in membrane trafficking (Lee et al., 2002; Patel and Latterich, 1998; Lupas and Martin, 2002), it

is tempting to speculate that intracellular transportation regulated through these proteins is an important factor in plant defense systems.

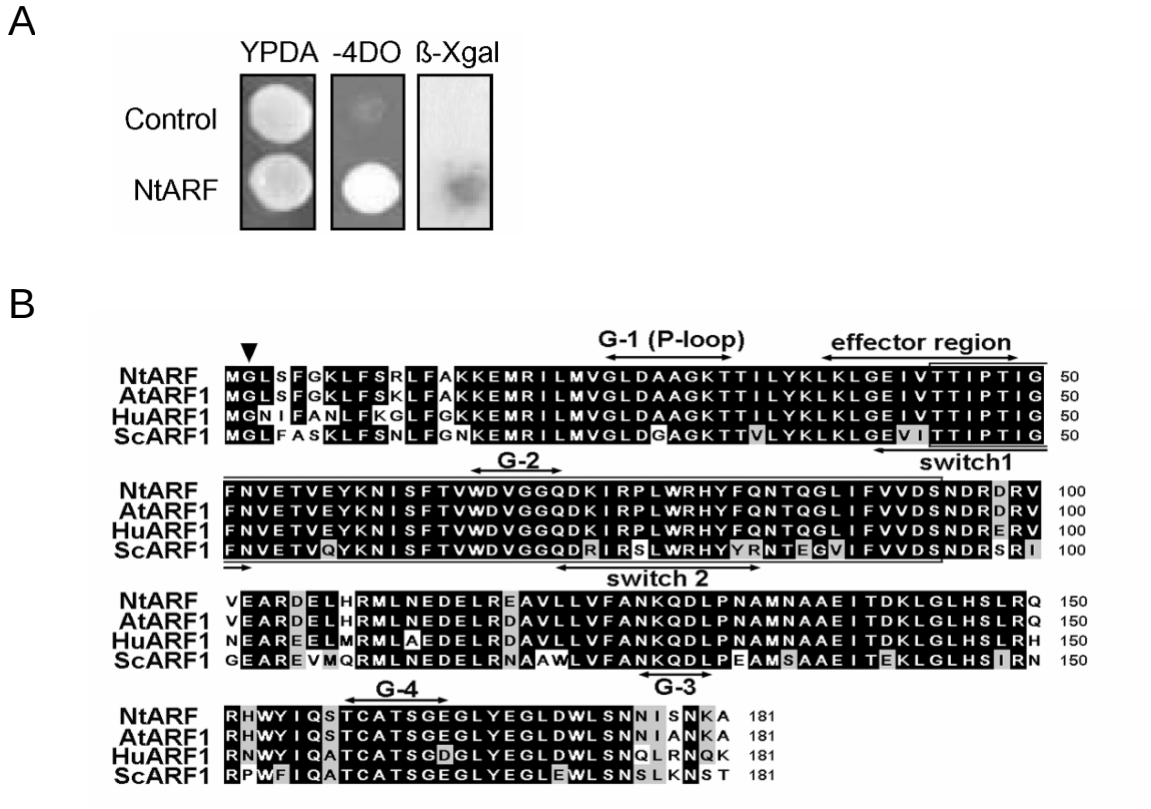

Figure 7. Isolation of NtAAA1 interacting factor.

(A)Yeast two-hybrid screening of a tobacco cDNA library using *NtAAA1* as the bait. Yeast Y187 cells were transformed with *NtAAA1* and mated to a host strain (AH109) containing the library. Colonies were selected on SD agar supplemented with amino acid mixture depleted of histidine, tryptopan and leucine, adenine (-4DO). One particular clone (NtARF) was finally obtained and subjected to β-galactosidase assay (β-Xal). Assay with an empty vector was used as control. (B) Amino acid sequence alignment. NtARF (accession no. AB274306) is aligned with ARF proteins from Arabidopsis (CAB95166) (AtARF1), *Home sapiens* (P32889) (HsARF1) and *Saccharomyces cerevisiae* (P11076) (ScARF1). The conserved GTP binding motifs are indicated by G-1 (P-loop), G-2, G-3 and G-4, and interacting regions with GEF sec7 domains are indicated by switch 1 and switch 2. The effector region is the binding site with GAPs (Gebbie *et al.*, 2005), and myristoylation site at the N-terminus is shown by a closed arrowhead. Amino acid residues between positions 35 and 94 (indicated by a large box) are required for binding to phospholipase D and adaptor protein AP-1.

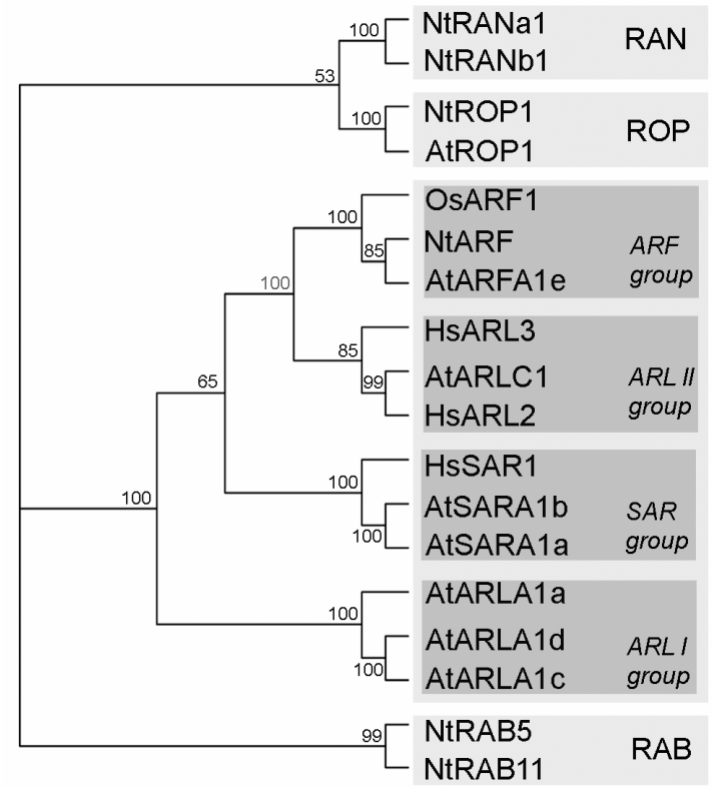

Figure 8. Phylogenetic analysis of *NtARF*.

Amino acid sequences were aligned using the neighbour-joining method in CLUSTALW and displayed using the TREEVIEW program. The tree was rooted with the other GTPase, RAN, ROP and RAB, and branches with percentage bootstrap values were indicated. Samples are from Arabidopsis (At), humans (*Homo sapiens*, Hs), rice (*Oryza sativa*, Os). Accession numbers are NtARF (BAF34209), AtARFA1e (CAB71889), OsARF1 (AF012896); AtARLA1a (BAB08314), AtARL1d (BAB 08464), AtARLA1c (CAB66925); HsARL2 (AAH02530), AtARLC1 (AAD15498), HsARL3 (CAG28565); AtSARA1a (AC003114), AtSARA1b (AC069159), HsSAR1 (CAG38523); NtRANa1 (P41918), NtRANb1 (P41918); NtRAB5 (P29687) NtRAB11 (Q40521); NtROP1 (CAA10815), AtROP1 (NP 190698). ARF GTPase are grouped into four distinct families, ARF, SAR, ARL I and ARL II.

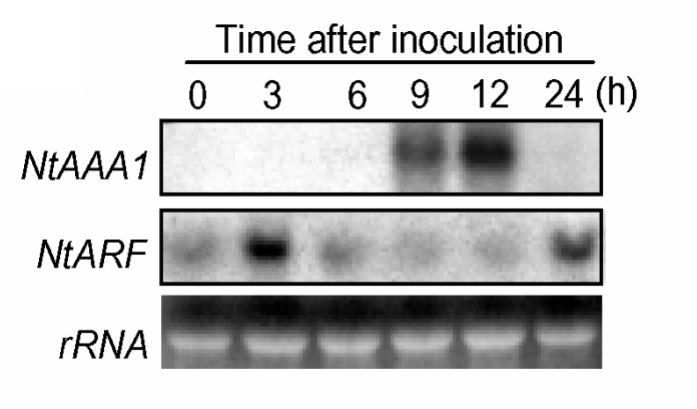

Figure 9. Transcript accumulation upon pathogen infection.

Healthy leaves from wild type plants were inoculated with *P. syringae* pv *glycinea* and incubated for indicated time period. Total RNA was extracted and subjected to RNA blot analysis with probe cDNAs for *NtAAA1* (upper panel) and *NtARF* (middle panel). For loading standard, rRNA is shown (lower panel).

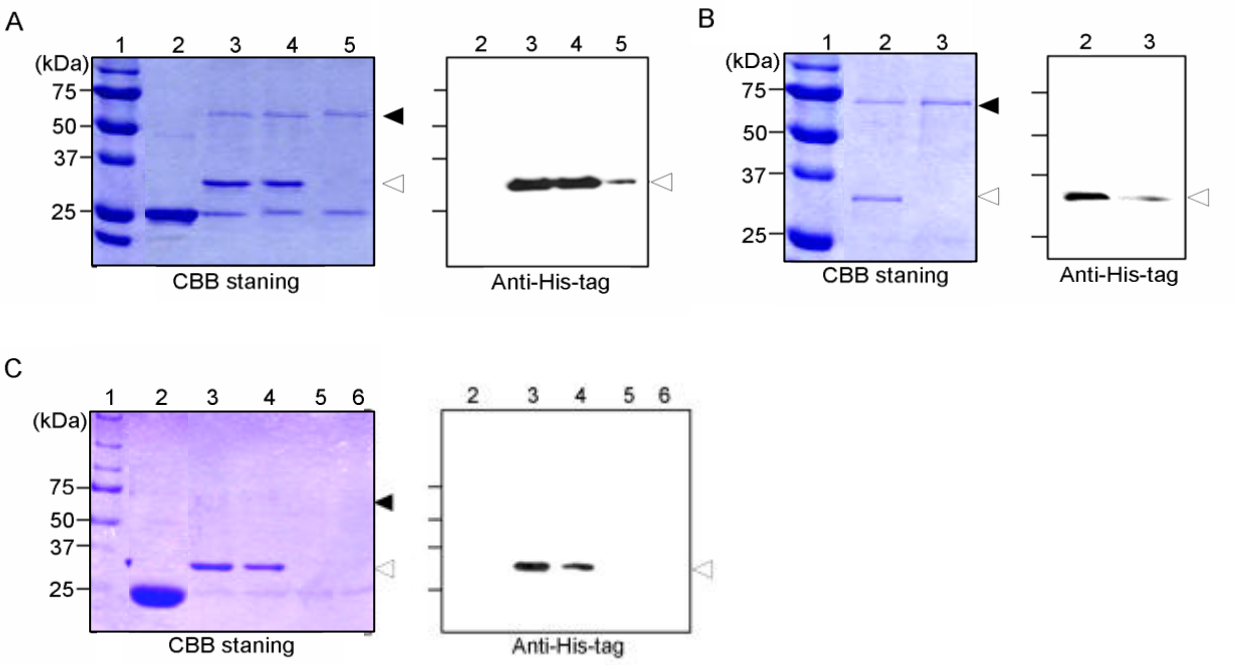

Figure 10. Interaction between NtAAA1 and NtARF.

(A) In vitro interaction between of NtAAA1 and NtARF derivatives. Purified His-tagged NtARF (lane 3), His-tagged NtARF^{Q71L} (active form, lane 4) or His-tagged NtARF^{T31L} (inactive form, lane 5) were incubated with GST-tagged NtAAA1 coupled to GSH resin, washed and eluted with reduced glutathione solution. As the control, purified GST (lane 2) was subjected to NtARF binding. Eluates were fractionated on SDS-PAGE, stained with Coomasie brilliant blue (CBB staining), then blotted to immobilon sheet, which was subjected to immuno-blot assay with antibodies against His (Anti-His-tag). Closed and open arrowheads indicate the position of GST-NtAAA1 and His-NtARF, respectively. Molecular markers are shown in lane 1. (B) Preferential binding of NtAAA1 to GTP-bound NtARF. His-tagged NtARF was preincubated with either GTP[γS] (lane 2) or GDP[βS] (lane 3) prior to binding to NtAAA1, and then subjected to pull-down assay as described above. Positions of GST-tagged NtAAA1 and His-tagged NtARF are indicated by closed and open arrowheads, respectively. Molecular markers are shown in lane 1. (C) Preferential binding of NtARF to ATP-bound NtAAA1. GST-tagged NtAAA1 was preincubated with either ATP[γS] or ADP[βS] prior to binding to His-tagged NtARF, His-tagged NtARF^{Q71L} or His-tagged NtARF^{T31L} and then subjected to pull-down assay as described in the legend for figure 4c. Binding combinations were; GST and His-tagged NtARF as the control (lane2), GST-tagged NtAAA1 preincubated with ATP[γS] and His-tagged NtARF^{Q71L} (lane 3), GST-tagged NtAAA1 preincubated with ADP[βS] and His-tagged NtARF^{Q71L} (lane 4), GST-tagged NtAAA1 preincubated with ATP[γS] and His-tagged NtARF^{T31L} (lane 5), and GST-tagged NtAAA1 preincubated with ADP[βS] and His-tagged NtARF^{T31L} (lane 6). Molecular markers are shown in lane 1.

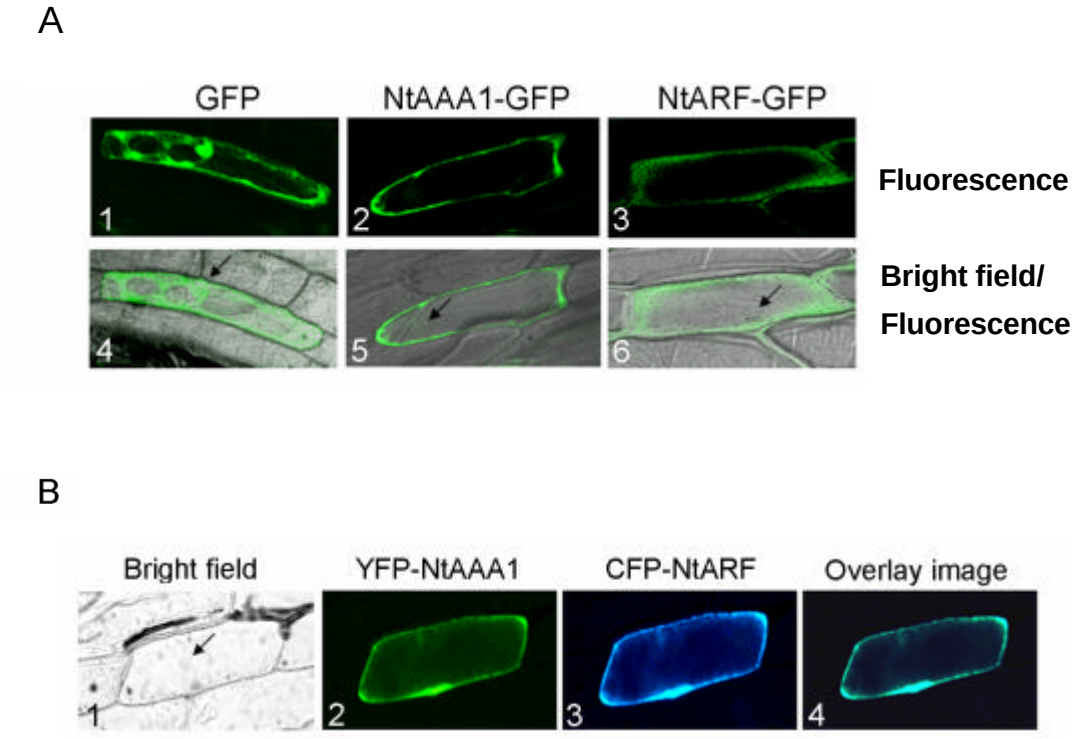

Figure 11. Intracellular localization and physical interaction.

(A) Intracellular localization. Onion epidermal cell layers were bombarded with gold particles coated with GFP alone (1, 4), NtAAA1-GFP (2, 4) or NtARF-GFP (3, 6) and observed by epifluorescence of GFP (1, 2, 3) (fluorescence). Fluorescence and bright field images were merged (4, 5, 6) (Bright field/ fluorescence). (B) Co-localization. Onion epidermal cell layers were bombarded with gold particles coated with *YFP-NtAAA1* and *CFP-NtARF* expression vectors, and fluorescence observed at 514 nm for YFP (2) or CFP (3) at 458 nm under microscope. Images under bright field (1) and overlay of YFP and CFP fluorescence (2) are also shown.

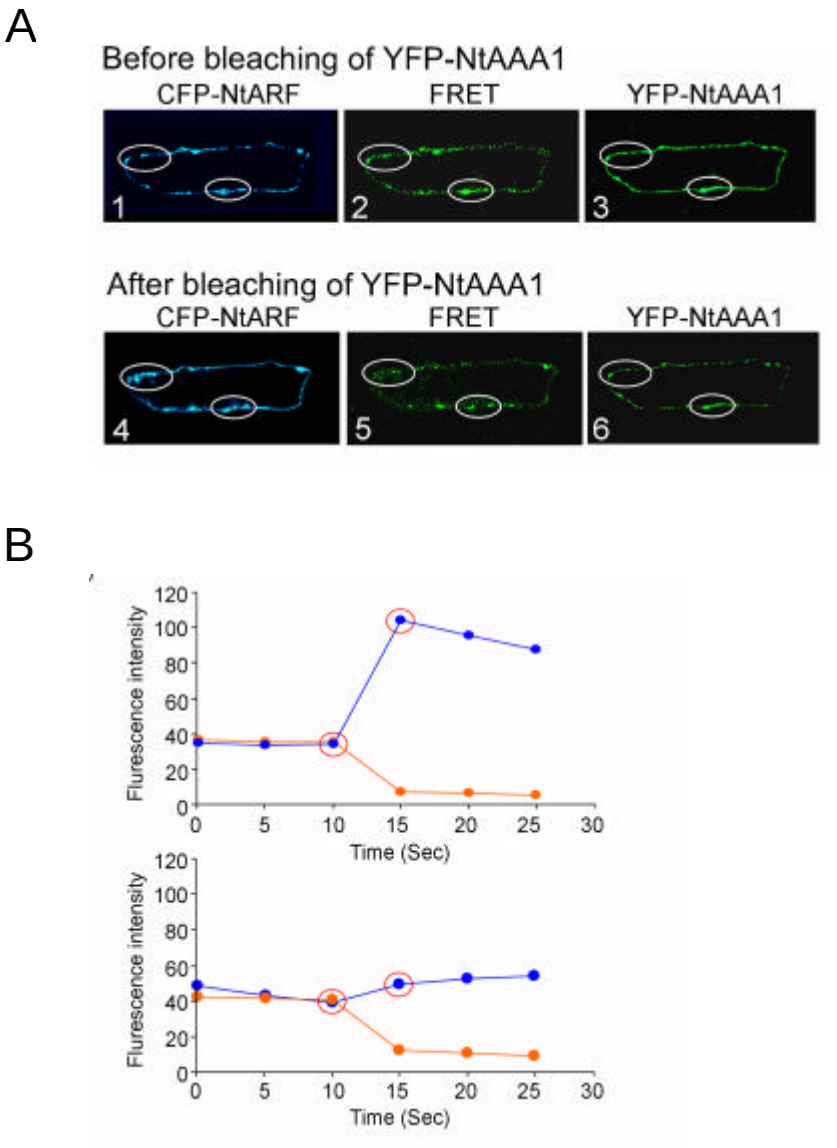

Figure 12. FRET analysis.

(A) Accepter photobleaching analysis. Onion epidermal cell layers were bombarded with gold particles coated with *YFP-NtAAA1* and *CFP-NtARF* expression vectors, and observed before (upper panel) and after (lower panel) photobleaching. White circles indicate the region of interest (ROI). (B) Quantification of fluorescence. Donor and the acceptor fluorescence intensities at different time points before and after acceptor photobleaching were measured. The red circles show the start (10 sec) and end (15 sec) of the bleach cycle.

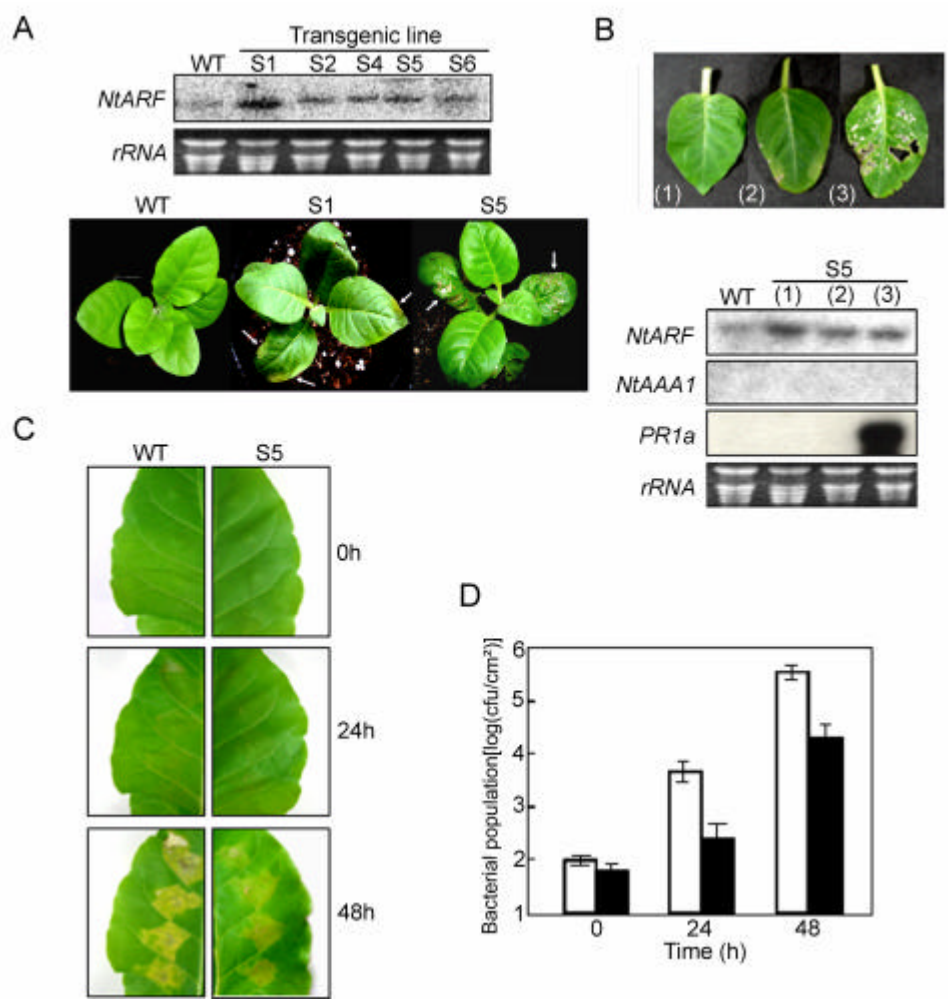

Figure 13. Properties of transgenic tobacco plants constitutively expressing *NtARF*.

(A) Expression of introduced gene and phenotypes. RNA blot analysis of wild-type (WT) and *NtARF* over-expressing transgenic plants (S1, S2, S4 through S6) (upper panel). Whole view of 2-month old wild type (WT) and transgenic lines (S1 and S5). Note that lesions appeared only in aged leaves. (B) Expression of *NtARF*, *NtAAA1* and *PR-1a* in young leaf (1), aged leaf without lesion (2) or aged leaf with lesion (3) from transgenic S5 plants (S5). Total RNA was isolated from these leaf samples, and subjected to RNA blot analysis using indicated probe cDNAs. (C) Lesion development. Leaves of wild-type (WT) or transgenic S5 line (S5) were inoculated with *P. syringae* pv *glycinea*, and symptoms were observed at indicated time points. (D) Bacterial population in inoculated regions. Leaf discs from wild-type (open bar) or transgenic S5 line (S5) (closed bar) were collected at indicated time point after infection and subjected to bacteria counting. Values are from triplicate measurements with standard deviation and expressed in logarithmic scale.

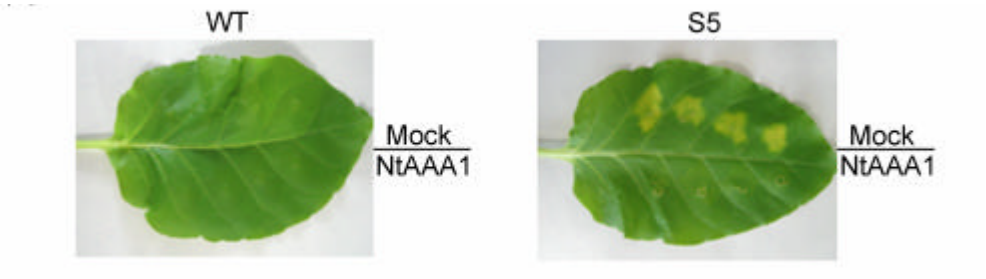

Figure 14. Wound response of *NtARF* overexpressing tobacco leaves.

Effect of transient expression of *NtAAA1* on wound response. A healthy leaf from wild type (WT) or *NtARF* over-expressing transgenic plant (S5) was cut off and subjected to infiltration with *Agrobacterium* containing *NtAAA1*-expression vector (NtAAA1) or empty control vector (Mock). Infiltrated leaf was incubated at 23°C for 5 days and photographed. Note that infiltrated area was wounded due to micro syringe attachment.

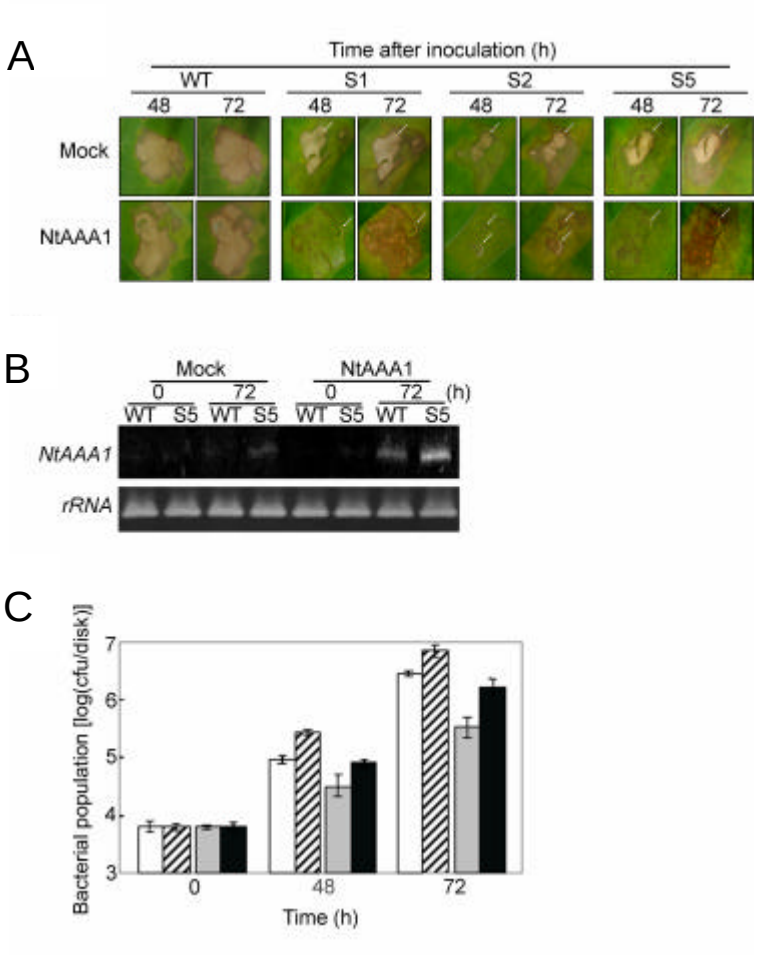

Figure 15. Pathogen response of *NtARF* overexpressing tobacco leaves.

(A) Effect of transient expression of *NtAAA1* on pathogen response. A healthy leaf from wild type (WT) or *NtARF* over-expressing transgenic lines (S1, S2 and S5) was cut off and simultaneously infiltrated with *P. syringae* pv. *glycine* and *Agrobacterium* harboring *NtAAA1*-expression vector (NtAAA1) or empty control vector (Mock). Infiltrated leaf was incubated at 23°C for indicated time period and photographed. Arrows indicate touching positions of syringe for infiltration. (B) Transcript accumulation of *NtAAA1*. Infiltrated leaves as described above were punched with a paper puncher after 0 or 74 h after infiltration, and RNA samples were reverse-transcribed with oligo$(dT)_{18}$, and amplified with specific primers for *NtAAA1* or *rRNA*. Products were fractionated on agarose gel electrophoresis, and visualized by ethidium bromide staining. (C) Bacterial population in inoculated regions. Leaf discs from wild-type or transgenic S5 line were collected at indicated time point after infection and subjected to *P. syringae* pv. *glycine* counting on KB plate by incubation at 25°C for 24 h. Note that *Agrobacterium* does not grow on KB plate. Samples were from mock-treated wild type disc (open bar), *NtAAA1*-expressing wild type disc (hatched bar), mock-treated transgenic S5 disc (shaded bar), and *NtAAA1*-expressing transgenic S5 disc (closed bar). Values are from triplicate measurements with standard deviation and expressed in logarithmic scale.

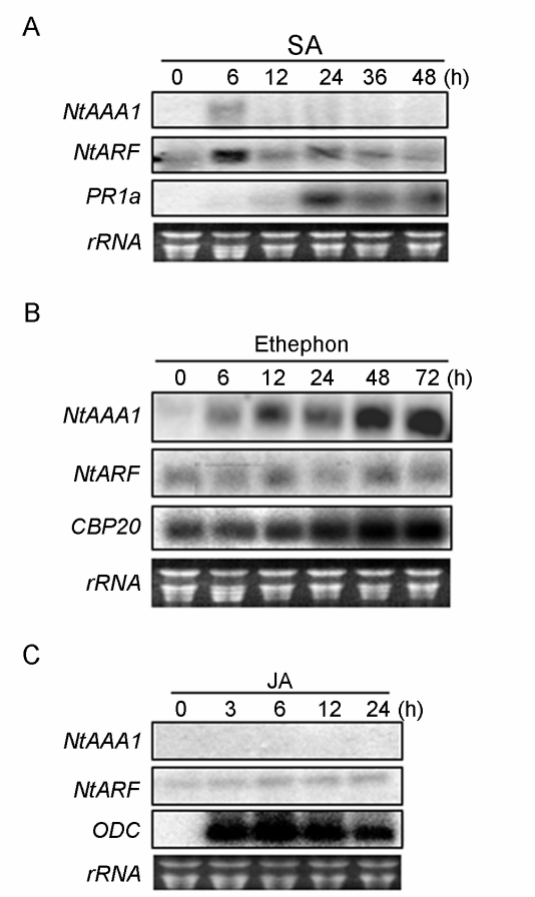

Figure 16. Phytohormone response of *NtAAA1* and *NtARF*.

Detached healthy leaves of wild type tobacco (*N. tabacum* cv. *Xanthi* NN) were left for 4 h for acclimatization to the initial wound stress, and then subjected to treatment with 1 mM SA (A), 100 μM ethephon (B) or 50 μM JA (C). Total RNA was isolated from leaves at indicated time points, and 20 μg aliquot per lane was fractionated on agarose gel electrophoresis, transferred to nylon membrane and subjected to hybridization with indicated cDNA probes. As the positive controls to confirm efficiency of phytohormone treatments, cDNA probes for SA-responsive *PR1a* (*PR1a*), ethylene-responsive *CBP20* (*CPB20*) and JA-responsive ornithine decarboxylase (*ODC*) were used in parallel. For equal loading of RNA samples, rRNA was used (lower panel).

CONCLUSION REMARKS

Two main contributions of this study are:

(1) NtAAA1 protein acts as a negative regulator of the SA signaling pathway in defense response.

(2) NtAAA1 specifically interacts with NtARF and reduces its resistant activity against pathogen attack.

NtAAA1-RNAi transgenic plans were found to exhibit an elevated resistance to *Pseudomonas syringae* infection in comparison with wild type plants, suggesting that NtAAA1 negatively controlled the defense reaction. Subsequently, I performed micro-array analysis to screen for genes which were under the control of NtAAA1 using transgenic *NtAAA1*-RNAi plants. Analysis of identified genes suggested that NtAAA1 might act as a negative regulator of the SA signaling pathway by mediating the JA signals. Since AAA proteins are considered to function through protein-protein interactions, NtAAA1-interacting protein was screened by the yeast two-hybrid assay, and a small GTPase, an ADP ribosylation factor was identified. Characterization of NtARF indicated that:

(i) Interaction predominantly occurrs between active forms of NtAAA1 in ATP-bound and NtARF in GTP-bound forms

(ii) Transcripts of *NtARF* are rapidly induced upon bacteria infection.

(iii) *NtARF* overexpressing transgenic plants exhibit spontaneous and wound-induced lesion formation.

(iv) NtARF plays a positive role in defense responses.

(v) NtAAA1 interferes with NtARF, and reduces its function.

(vi) NtAAA1 and NtARF may partly be responsible for antagonistic actions between JA and/or ethylene and SA in defense response.

As the conclusion of this study, I summarize in the following diagram (Figure 17). Upon pathogen infection, plant signaling substances such as, SA, JA and ethylene, are produced. Transcription of *NtARF* is rapidly induced by SA. Newly synthesized ARF protein is activated into GTP-bound form by guanine-exchange factors (GEFs), and in turn switches on resistance response. *NtAAA1* is induced at later phases by ethylene, and possibly activated into ATP-bound form by a JA induced protein, of which identification must be determined. Upon complex formation between GTP bound-NtARF and ATP bound-NtAAA1 proteins, ARF-induced resistance response is switched off resulting in adjustment of resistance level to appropriate level. This model proposes a self-regulated circuit in plant defense by operating both acceleration and brake of the HR.

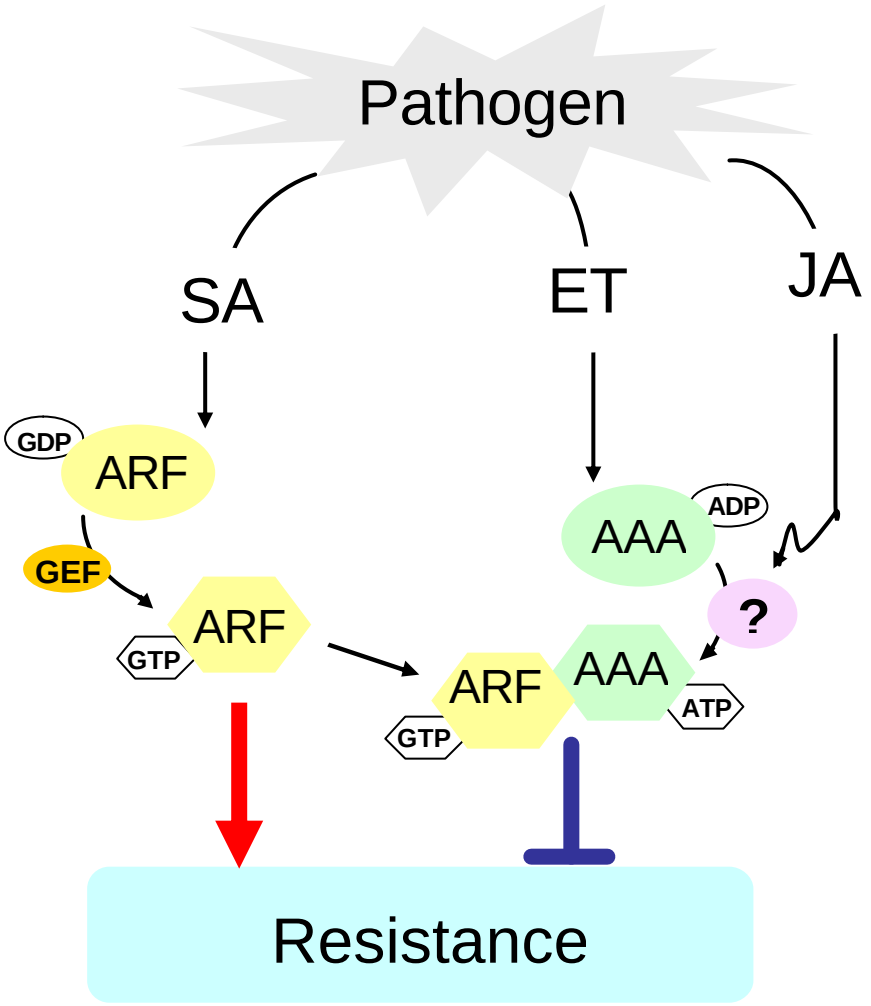

Figure 17. Model for AAA –ARF interactions during pathogen response.

References

Baker, B., Zambryski, P., Staskawicz, B., and Dinesh-Kumar, S.P. (1997). Signaling in plant-microbe interactions. Science 276, 726-733.

Birschmann, I., Rosenkranz, K., Erdmann, R., and Kunau, W.H. (2005). Structural and functional analysis of the interaction of the AAA-peroxins Pex1p and Pex6p. FEBS J. 272, 47-58.

Botos, I., Melnikov, E.E., Cherry, S., Khalatova, A.G., Rasulova., F.S., Tropea, J.E., Maurizi, M.R., Rotanova, T.V., Gustchina, A., and Wlodawer, A. (2004). Crystal structure of the AAA^{+}adomain of E.coli Lon protease at 1.9Å resolution. J. Struct. Biol. 146, 113-122.

Bourne, H.R., Sanders, D.A., and McCormick, F. (1991). The GTPase super-family: conserved structure and molecular mechanism. Nature 349, 117-127.

Bradford, M.M. (1976). A rapid and sensitive method for the quantification of microgram quantities of protein utilizing the principle of dye-binding. Anal. Biochem. 72, 248-254.

Chomczynski. P., and Sacchi, N. (1987). Single-step method of RNA isolation by acid guanidinium thiocyanate-phenol-chloroform extraction. Anal. Biochem. 162, 156-159.

Clarke, J.D., Liu, Y., Klessing, D.F., and Dong, X. (1998). Uncoupling PR gene expression from NPR1 and bacterial resistance: characterization of the dominant Arabidopsis *cpr6-1* mutant. Plant Cell 10, 557-569.

Clarke, J.D., Volko, S.M., Ledford, H., Ausubel, F.M., and Dong, X. (2000). Role of salicylic acid, jasmonic acid, and ethylene in *cpr*-induced resistance in Arabiposis. Plant Cell 12, 2175-2190.

Confalonieri, F., and Duguet, M. (1995). A 200-amino acid ATPase module in search of a basic function. Bioessays 17, 639-650.

Dascher, C., and Balch, W.E. (1994). Dominant inhibitory mutants of ARF1 block endoplasmic reticulum to golgi transport and trigger disassembly of the golgi apparatus. J. Biol. Chem. 269, 1437-1448.

Devoto, A., and Turner, J.G. (2003). Regulation of jasmonate-mediated plant response in Arabidopsis. Annals Bot. 92, 329-337.

Doares, S.H., Narváez-vásquez, J., Conconi, A., and Ryan, C.A. (1995). Salicylic acid inhibits synthesis of proteinase-inhibitors in tomato leaves induced by systemic and jasmonic acid. Plant Physiol.108, 1741-1746.

Doherty, H.M., Selvendran, R.R., and Bowles, D.J. (1988). The wound response of tomato plants can be inhibited by aspirin and related hydroxylbenzoic acids. Physiol. Mol. Plant Pathol. 82, 647-651.

Donaldson, J.G. (2000). Filling in the GAPs in the ADP-ribosylation factor story. Proc. Natl Acad. Sci. 97, 3792-3794.

Felton, G.W., Korth, K.L., Bi, J.L., Wesley, S.V., Huhman, D.V., Mathews, M.C., Murphy,

J.B., Lamb, C., and Dixon, R.A. (1999). Inverse relationship between systemic resistance of plants to microganisms and to insect herbivory. Curr. Biol. 9, 317-320.

Felton, G..W., and Korth, K.L. (2000). Trade-offs between pathogen and herbivore resistance. Curr. Opin. Plant Biol. 3, 309-314.

Fu, H., Doelling, J.H., Rubin, D.M., and Vierstra, R.D. (1999). Structural and functional analysis of the six regulatory particle triple-A ATPase subunits from the Arabidopsis 26S proteasome. Plnat J. 18, 529-539.

Glazebrook, J. (1999). Genes controlling expression of defense responses in Arabidopsis. Curr. Opin. Plant Biol. 2, 280-286.

Goodman, R.N., and Novacky, A.J. (1994). The Hypersensitive Reaction in Plants to Pathogens: A Resistance Phenomenon, (St. Paul: American Phytopathological Society Press)

Gupta, V., Willits, M.G., and Glazebrook, J. (2000). Arabidopsis thaliana EDS4 contributes to salicylic acid (SA)-dependent expression of defense responses: evidence for inhibition of jasmonic acid signaling by SA. Mol. Plant Microbe Interact. 13, 503-511.

Hammond-Kosack, K.E., and Jones, J.D.G. (1996). Resistance gene-dependent plant defense responses. Plant Cell 8, 17773-1791.

Hammond, S.M., Altshuller, Y.M., Sung, T.C., Rudge, S.A., Rose, K., Engebrecht, J., Morris,

A.J., and Frohman, M.A. (1995). Human ADP-ribosylation factor-activated phosphatidylcholine-specific phospholipase D defines a new and highly conserved gene family. J. Biol. Chem. 270, 29640-29643.

Jirage, D., Zhou, N., Cooper, B., Clarke, J.D., Dong, X., and Glazebrook, J. (2001). Constitutive salicylic acid-dependent signaling in cpr1 and cpr6 mutants requires PAD4. Plant J. 26, 395-407.

Jones, D.H., Bex, B., Fensome, A., and Cockcroft, S. (1999). ADP-ribosylation factor 1 mutants identify a phospholipase D effector region and reveal that phosholipase D participates in lysosomal secretion but is not sufficient for recruitment of coatomer I. Biochem. J. 341, 185-192.

Jou, Y., Chiang, C.P., Jauh, G.Y., and Yen, H.E. (2006). Functional characterization of Ice Plant SKD1, an AAA-type ATPase associated with the Endoplasmic reticulum-golgi network, and its role in adaptation to salt stress. Plant Physiol. 141, 135-146.

Kahn, R.A., and Gilman, A.G. (1986). The protein cofactor necessary for ADP-ribosylation of Gs by cholera toxin is itself a GTP binding protein. J. Biol. Chem. 261, 7906-7911.

Kanoh, H., Williger, B.T., and Exton, J.H. (1997). Arfaptin 1, a putative cytosolic target protein of ADP-ribosylation factor, is recruited to golgi membranes. J. Biol. Chem. 272, 5421-5429.

Katoh, A., Yamaguchi, Y., Sano, H., and Hashimoto, T. (2003). Analysis of expression

sequence tags from Nicotiana sylvestris. Proc. Japan Acad. 79, 151-154.

King, E.O., Ward, M.L., and Raney, D.E. (1954). Two simple media for the demonstration of pyocyanin and fluorescein. J. Lab. Clin. Med. 22, 301-307.

Laudert, D., and Weiler, E.W. (2002). Allene oxide synthesis: a major control point in *Arabidopsis thaliana* octadecanoid signaling. Plnat J. 15, 675-684.

Lee, M.H., Min, M.K., Lee, Y.J., Jin, J.B., Shin, D.H., Kim, D.H., Lee, K.H., and Hwang, I. (2002). ADP-ribosylation factor 1 of Arabidopsis plans a critical role in intracellular trafficking and maintenance of endoplasmic reticulum morphology in Arabidopsis. Plant Physiol. 129, 1507-1520.

Lee, W.Y., Hong, J.K., Kim, C.Y., Chun, H.J., Park, H.C., Kim, J.C., Yun, D.J., Chung, W.S., Lee, S.H., Lee, S.Y., Cho, M.J., and Lim, C.O. (2003). Over-expressed rice ADP-ribosylation factor 1 (RARF1) induces pathogenesis-related genes and pathogen resistance in tobacco plants. Physiol. Plant. 119, 573-581.

Lindahl, M., Tabak, S., Cseke, L., Pichersky, E., Andersson, B., and Adam, Z. (1996). Identification, characterization, and molecular cloning of a homologue of the bacterial FtsH protease in chloroplasts of higher plants. J. Biol. Chem. 271, 29329-29334.

Liscovitch, M., Chalifa, V., Pertile, P., Chen, C.S., and Cantley, L.C. (1994). Novel function of phosphatidylinositol 4,5-bisphosphate as a cofactor for brain membrane phospholipase D. J. Biol. Chem. 269, 21403-21406.

Lupas, A.N., and Martin, J. (2002). AAA proteins. Curr. Opin. Struct. Biol. 12, 746-753.

McElver, J., Patton, D., Rumbaugh, M., Liu, C.M., Yang, L.J., and Meinke, D. (2000). The TITAN5 gene of Arabidopsis encodes a protein related to the ADP-ribosylation factor family of GTP binding proteins. Plant Cell 12, 1379-1392.

Moss, J., and Vaughan, M. (1995). Structure and function of ARF proteins: Activators of cholera toxin and critical components of intracellular vesicular transport processes. J. Biol. Chem. 270, 12327-12330.

Mur, L.A., Brown, I.R., Darby, R.M., Bestwick, C.S., Bi, Y.M., Mansfield, J.W., and Draper, J. (2000). A loss of resistance to avirulent bacterial pathogens in tobacco is associated with the attenuation of a salicylic acid-potentiated oxidative burst. Plant J. 23, 609-621.

Mur, L.A.J., Bi, Y.M., Darby, R.M., Firek, S., and Draper, J. (1997). Compromising early salicylic acid accumulation delays the hypersensitive response and increases viral dispersal during lesion establishment in TMV-infected tobacco. Plant J. 12, 1113-1126.

Mur, L.A.J., Kenton, P., Atzorn, R., Miersch, O., and Wasternack, C. (2006). The outcomes of concentration-specific interactions between salicylate and jasomate signaling include synergy, antagonism and oxidative stress leading to cell death. Plant Physiol. 140, 249-262.

Mysore, K.S., and Ryu, C.M. (2004). Nonhost resistance: how much do we know? Trends Plant Sci. 9, 97-104.

Nie, Z., Hirsh, D.S., and Randazzo, P.A. (2003). Arf and its many interactors. Curr. Opin. Cell Biol. 15, 396-404.

Niki, T., Mitsuhara, I., Seo, S., Ohtsubo, N., and Ohashi, Y. (1998). Antagonistic effect pathogenesis-related (PR) protein genes in wounded mature tobacco leaves. Plant Cell Physiol. 39, 500-507.

Numberger, T., and Brunner, F. (2002). Innate immunity in plants and animals: emerging parallels between the recognition of general elicitors and pathogen associated molecular pattems. Curr. Opin. Plant Biol. 5, 318-324.

Olsen, L.J. (1998). The surprising complexity of peroxisome biogenesis. Plant Mol. Bio. 38, 163-189.

Orci, L., and Palmer, D.J. (1993). Budding of Golgi membranes requires the coatomer complex of non-clathrin coat proteins. Nature 362, 648-652.

Patel, S., and Latterich, M. (1998). The AAA team: related ATPases with diverse functions. Trends Cell Biol. 8, 65-71.

Petersen, M., Brodersen, P., Naested, H., Andreasson, E., Lindhart, U., Johansen, B., Nielsen, H.B., Austin, M.J., Parker, J.E., et al., (2000). Arabidopsis MAP kinase 4 negatively regulates systemic acquired resistance. Cell 103, 1111-1120.

Piterse, C.M.J., and van Loon, L.C. (1999). Salicylic acid independent plant defence pathways. Trends Plant Sci. 4, 52-58.

Rancour, D.M., Dickey, C.E., Park, S., and Bednarek, S.Y. (2002). Characterization of ATCDC48. Evidence for multiple membrane fusion mechanisms at the plane of cell division in plants. Plant Physiol. 130, 1241-1253.

Rechsteiner, M., Iioffman, L., and Dubiel, W. (1993) The multicatalytic and 26S proteases. J Biol. Chem. 268, 6065-6068.

Ritzenthaler, C., Nebenführ, A., Movafeghi, A., Stussi-Garaud, C., Behnia, L., Pimpl, P., Staehelin, L.A., and Robinson, D.G. (2002). Reevaluation of the effects of brefeldin A on plant cells using tobacco Bright Yellow 2 cells expression Golgi-targeted green fluorescrent protein and COPI antisera. Plant Cell 14, 237-261.

Ryals, J.A., Neuenschwander, U.H., Willits, M.G., Molina, A., Steiner, H.Y., and Hunt, M.D. (1996). Systemic acquired resistance. Plant Cell 8, 1809-1819.

Seo, S., Okamoto, M., Iwai, T., Iwano, M., Fukui, K., Isogai, A., Nakajima. N, and Ohashi, Y. (2000). Reduced level of chloroplast FtsH protein in tobacco mosaic virus-infected tobacco leaves accelerate the hypersensitive reaction. Plant Cell 12, 917-932.

Shirasu, K., Nakajima, H., Rajasekhar, V.K., Dixon, R.A., and Lamb, C. (1997). Salicylic acid potentiates an agonist-dependent gain control that amplifies pathogen signals in the activation of defense mechanisms. Plant Cell 9, 261-270.

Sieburth, L.E., Muday, G.K., King, E.J., Benton, G., Kim, S., Metcalf, K.E., Meyers, L., Seamen, E., and Van Norman J.M. (2006). SCARFACE encodes an ARF-GAP that is required for normal auxin efflux and vein patterning in Arabidopsis. Plant Cell 18,

1392-1411.

Song, X.F., Yang, C.Y., Liu, J., and Yang, W.C. (2006). RPA, a class II ARFGAP protein, activates ARF1 and U5 and plays a role in root hair development in Arabidopsis. Plant Physiol. 141, 966-976.

Spoel, S.H., Koornneef, A., Claessens, S.M., Korzelius, J.P., Van Pelt, J.A., Mueller, M.J., Buchala, A.J., Metraux, J.P., Brown, R., Kazan, K., van Loon, L.C., Dong, X., and Pieterse, C.M.J. (2003). NPR1 modulates cross-talk between salicylate- and jasmonate-dependent defense pathways through a novel function in the cytosol. Plant Cell 15, 760-770.

Sugimoto, M., Yamaguchi, Y., Nakamura, K., Tatsumi, Y., and Sano, H. (2004). A hypersensitive response-induced ATPase associated with various cellular activities (AAA) protein from tobacco plants. Plant Mol. Biol. 56, 973-985.

Taguchi, F., Shimizu, R., Nakajima, R., Yoyoda, K., Shiraishi, T., and Ichinose, Y. (2003). Differential effects of flagellins from *Pseudomonas syringae* pv. *tabaci*, *tomato* and *glycinea* on plant defense response. Plant Physiol. Biochem. 41, 165-174.

Takeuchi, K., Taguchi, F., Inagaki, Y., Toyoda, K., Shiraishi, T., and Ichinose, Y. (2003). Flagellin glycosylation island in *Pseudomonas syringae* pv. *glyciena* and its role in host specificity. J. Bacteriol. 185, 6658-6665.

Thordal-Christensen, H., Zhang, Z., Wei, Y., and Collinge, D.B. (1997). Subcellular localization of H_2O_2 in plnats: H_2O_2 accumulation in papillae and hypersensitive

response during the barley-powdery mildew interaction. Plant J. 11, 1187-1194.

Thordal-Christensen, H. (2003). Fresh insights into processes of nonhost resistance. Curr. Opin. Plant Biol. 6, 351-357.

Turner, C.E., and Brown, M. (2001). Cell motility : ARNO and ARF6 at the cutting edge. Curr. Biol. 11, R875-R877.

Ueda, H., Yamaguchi, Y., and Sano, H. (2006). Direct interaction between the tobacco mosaic virus helicase domain and the ATP-bound resistacne protein, N factor during the hypersensitive response in tobacco plants. Plant Mol. Biol. 61, 31-45.

Vale, R.D. (2000). AAA proteins: Lords of the ring. J. Cell Biol. 150, F13-F19.

Vernoud, V., Horton, A.C., Yang, Z., and Nielsen, E. (2003). Analysis of the small GTPase gene superfamily of Arabidopsis. Plant Physiol. 131, 1119-1218.

Von Arnim, A.G., Deng, X.W., and Stacey, M.G. (1998). Cloning vectors for the expression of green fluorescent protein fusion protein in transgenic plants. Gene 221, 35-43.

Waller, F., Müller, A., Chung, K.M., Yap, Y.K., Nakamura, K., Weiler, E. and Sano, H. (2006). Expression of a WIPK-activated transcription factor results in increase of endogenous salicylic acid and pathogen resistance in tobacco plants. Plant Cell Physiol. 47, 1169-1174.

Wang, K.L.C., Li, H., and Ecker, J.R. (2002). Ethylene biosynthesis and signaling networks.

Plant Cell S131-S151.

Yang, Y., Shah, J., and Klessing, D.F., (1997). Signal perception and transduction in plant defense responses. Genes Dev. 11, 1621-1639.

Yap, Y.K., Kakamu, K., Yamaguchi, Y., Koizumi, N., and Sano, H. (2002). Promoter analysis of WIPK, a gene encoding a tobacco MAP kinase, with reference to wounding and tobacco mosaic virus infection. J. Plant Physiol. 159, 77-83.

Zerial, M., and Huber, L.A. (1995). Guidebook to the Small GTPases, (Oxford: Oxford University Press) pp. 429-453.

List of Publications

1. Lee, M.H., and Sano, H. (2007). Suppression of salicylic acid signaling pathways by an ATPase associated with various cellular activities (AAA) protein in tobacco plants. Plant Biotechnol. 24, 209-215.

2. Lee, M.H., and Sano, H. (2007). Attenuation of the hypersensitive response by an ATPase associated with various cellular activities (AAA) protein through suppression of a small GTPase, ADP ribosylation factor in tobacco plants. Plant J. (Accepted)

Acknowledgements

First, I would like to express my great gratitude to Professor Sano Hiroshi, for giving me an opportunity to study in Japan and for his continuous guidance and encouragement throughout this study. Special thanks is due to Professor Y.E. Choi (Kangwon national university, Korea) for continuous encouragement that enable me to carry out study in Japan. I wish to thank Dr. H. Yoda, Dr. M. Iwano, Ms. K-.M Chung, Ms. A. Yano (Nara Institute of Science and Technology) for helpful discussions, Dr. M. Sugimoto (Okayama University) for supplying the plasmids and transgenic plants, Dr. Moore, (Intermal Nagoya) for critical reading of manuscripts. I wish to thank Dr. Koizumi Nozomu, and all other member of the Laboratory of Plant Molecular Breeding (Nara Institute of Science and Technology) for their useful discussion and an enjoyable laboratory life. I am greatly in debt to the Japanese government for its financial support throughout my study. Finally, I am very grateful to my parents and partner, for continuous encouragement and support.

Appendix

Supplement Table 1-1. List of up-regulated genes in *NtAAA1* -RNAi plants.

	Clone ID	Putative funcion	Ration	P-value
stress and defense/21				
1	L-095_g0	Sar8.2b protein	3.22	0.02021
2	R-112_F0	putative Regulatory protein NPR1	1.58	0.01859
3	SOD		2.79	0.09843
4	L-095_g0	superoxide dismutase [Nicotiana plumbaginifolia]	2.01	0.04643
5	R-011_b1	putative translationally controlled tumor protein [Nicotiana tabacum]	1.5	0.12357
6	l-013_b04	putative translationally controlled tumor protein	1.52	0.34104
7	l-105_b01	salicylic acid binding catalase	1.81	0.00129
8	l-002_a11	putative translationally controlled tumor protein [Nicotiana tabacum]	2.91	0.00567
9	R-064_e0	isocitrate dehydrogenase (NAD+) [Nicotiana tabacum]	1.71	0.19457
10	R-016_c0	pleiotropic drug resistance like protein [Nicotiana tabacum]	2.01	0.5
11	L-096_e0	stress responsive protein homolog [Arabidopsis thaliana]	1.63	0.00046
12	L-010_c0	elicitor resposible protein [Nicotiana tabacum]	1.32	0.99998
13	L-098_c0	elicitor resposible protein [Nicotiana tabacum]	1.58	0.00167
14	R-057_c0	ACC oxidase [Nicotiana tabacum]	1.59	0.4562
15	R-044_A(	DnaJ-like protein [Arabidopsis thaliana]	1.5	0.07867
16	ACC oxidase		1.51	0.00102
17	l-011_d0	elicitor resposible protein [Nicotiana tabacum]	2.62	0.99479
18	l-013_e12	salicylic acid binding catalase	1.7	0.03181
19	l-093_b11	salicylic acid binding catalase	1.68	0.03158
20	l-031_e03	phospholipase D delta isoform 1a [Gossypium hirsutum]	1.81	0.09364
21	R-101_h0	ADP-ribosylation factor [Glycine max]	1.64	0.04317
transporte/6				
1	R-039_A(	vesicle transport v-SNARE	1.57	0.09364
2	l-001_e03	putative VAMP protein SEC22 [Arabidopsis thaliana]	1.56	0.02142
3	R-056_D(	putative equilibrative nucleoside transporter ENT3 [Arabidopsis thalian	1.7	0.99998
4	R-024_E(	mRNA export protein, putative [Arabidopsis thaliana]	1.88	0.0717
5	l-012_f02	vacuolar processing enzyme-1a [Nicotiana tabacum]	1.52	0.0407
6	R-021_A(	putative ABC transporter [Oryza sativa (japonica cultivar-group)]	1.62	0.05859
cell structure /7				
1	R-073_D	reversibly glycosylated polypeptide [Oryza sativa (japonica cultivar-gro	1.57	0.03091
2	R-040_f1	putative phytochelatin synthetase [Oryza sativa (japonica cultivar-group	1.79	0.11232
3	R-120_A(	extensin-like protein Dif54 [Lycopersicon esculentum]	2.35	0.00043
4	l-089_d03	alpha-tubulin [Gossypium hirsutum]	2.32	0.02261
5	R-101_f1	endomembrane protein 70, putative [Arabidopsis thaliana]	1.93	0.02167
6	L-076_E0	pectin methylesterase PME1 [Vitis vinifera]	2.02	0.77281
7	l-063_c05	P-Protein precursor [Flaveria trinervia]	1.65	0.31238
protein distribution and stoge/7				
1	R-068_c1	aspartic protease [Pyrus pyrifolia]	2.66	0.04251
2	L-041_F1	20S proteasome alpha 6 subunit [Nicotiana benthamiana]	2.56	0.03459
3	R-115_C(	putative AAA-metalloprotease [Oryza sativa (japonica cultivar-group)]	1.814	0.01564
4	L-046_E1	putative quinone reductase [Vitis vinifera]	2.09	0.64695
5	l-056_h0	similar to cdc2 protein kinase [Arabidopsis thaliana]	1.74	0.00436
6	l-088_f05	putative senescence-associated protein [Pisum sativum]	1.54	0.01943
7	l-019_g07	cysteine protease [Nicotiana tabacum]	1.66	0.01089
transciption/7				
1	l-108_c01	RNA helicase like protein DB10 [Nicotiana sylvestris]	2.66	0.95058
2	L-095_h0	putative eukaryotic translation initiation factor 6 [Oryza sativa (japonica	1.68	0.33424
3	L-095_g0	putative eukaryotic translation initiation factor 6 [Oryza sativa (japonica	1.98	0.17575
4	l-062_h0	transport protein particle component Bet3-like protein [Oryza sativa (ja	3.13	0.02998
5	l-108_c01	RNA helicase like protein DB10 [Nicotiana sylvestris]	1.5	0.63717
6	L-066_E0	elongation factor 1 alpha subunit [Malus x domestica]	2.89	0.50011
7	l-012_a12	elongation factor-1 alpha [Nicotiana tabacum]	1.55	0.28757

sinal transduction/1				
1	L-046_F0	signal recognition particle receptor protein [Cucumis sativus]	1.86	0.03985
secondary metaboli:/2				
1	R-103_d0	3-hydroxy-3-methylglutaryl-CoA reductase [Nicotiana attenuata]	2.62	0.02736
2	l-086_h0	acetyl Co-A acetyltransferase [Hevea brasiliensis]	2.48	0.60533
cell cycle:/1				
1	R-034_F0	carboxypeptidase C cbp31 [Oryza sativa (japonica cultivar-group)]	1.72	0.01809
metabolis /11				
1	R-011_f1	metallothionein-like protein	2.05	0.03354
2	R-018_E(	fatty acid alpha-oxidase [Oryza sativa]	1.68	0.01045
3	R-011_a0	ubiquitin carrier protein	1.84	0.20737
4	R-017_g0	metallothionein-like protein	3.77	0.59855
5	R-015_c0	metallothionein-like protein	2.1	0.50675
6	R-103_h0	hydroxymethylglutaryl coenzyme A synthase [Hevea brasiliensis]	1.96	0.04781
7	l-028_e0	Contains PF|00561 alpha/beta hydrolase fold. [Arabidopsis thaliana]	1.87	0.03091
8	l-017_g1	ubiquitin conjugating protein [Avicennia marina]	1.51	0.63567
9	R-105_H(	cyprosin [Cynara cardunculus]	1.55	0.03922
10	l-002_b0	ferredoxin-I [Lycopersicon esculentum]	1.68	0.00043
11	l-029_c1	39 kDa EF-Hand containing protein [Solanum tuberosum]	3.31	0.0328
energy /3				
1	L-037_E0	cytochrome c1 precursor [Solanum tuberosum]	2.53	0.01376
2	l-012_h0	PSI-D2 [Nicotiana sylvestris]	1.96	0.00696
3	L-098_h0	ribulose-1,5-bisphosphate carboxylase small subunit	2.44	0.00436
others /16				
1	R-011_d0	endomembrane protein 70, putative [Arabidopsis thaliana]	3.29	0.00677
2	R-068_h0	Putative FH protein interacting protein FIP1 [Oryza sativa (japonica cul	2.13	0.01512
3	R-016_f0	far-red impaired response protein (FAR1) [Arabidopsis thaliana]	2.04	0.03363
4	L-039_B(	putative ribosomal protein L10 [Arabidopsis thaliana]	1.81	0.02142
5	R-059_B(	putative 40S ribosomal protein S2 [Oryza sativa (japonica cultivar-grou	1.66	0.05027
6	R-010_g1	putative multiprotein bridging factor 1 [Nicotiana tabacum]	2.16	0.02022
7	l-105_b1	40S ribosomal protein S2 [Arabidopsis thaliana]	2.56	0.47585
8	l-094_c0	putative 60s ribosomal protein L37 [Arabidopsis thaliana]	1.99	0.00995
9	R-027_D(	putative nucleosome assembly protein [Arabidopsis thaliana]	1.69	0.04558
10	R-110_c0	putative multiprotein bridging factor 1 [Nicotiana tabacum]	2.01	0.03121
11	L-010_a0	putative 40S ribosomal protein s12	1.52	0.01106
12	l-001_e0	ribosomal protein L19 [Triticum aestivum]	1.6	0.20945
13	l-056_a0	putative ribosomal protein CtrL6e, 5'-partial [Oryza sativa (japonica cul	1.71	0.00255
14	R-055_B(	ribosomal protein L9 [Pisum sativum]	1.5	0.01769
15	l-001_f06	putative 40S ribosomal protein s12	1.52	0.03973
16	R-031_c0	tetratricopeptide repeat (TPR)-containing protein [Arabidopsis thaliana]	2.28	0.04178
unkown /9				
1	L-095_g04			
2	R-027_C12			
3	L-040_C12			
4	R-032_E09			
5	L-066_B08			
6	R-122_A05			
7	L-041_C04			
8	l-016_e12			
9	L-098_f08			

Supplement Table 1-2. List of down-regulated genes in *NtAAA1* -RNAi plants.

	Clone ID	Putative funcion	Ration	P-value
stress and defense /22				
1	l-	heat shock protein 70 [Nicotiana tabacum]	0.02	0.5
2	l-	putative stress protein [Arabidopsis thaliana]	0.015	0.0284
3	l-	glutathione S-transferase [Capsicum annuum]	0.15	0.03298
4	L-099_b1	secretory peroxidase [Nicotiana tabacum]	0.09	0.00097

5	L-006_F1	WRKY 12 [Theobroma cacao]	0.18	0.01045
6	R-026_G(	putative thioredoxin M [Arabidopsis thaliana]	0.3	0.03526
7	R-016_h0	dehydration stress-induced protein [Brassica napus]	0.31	0.59725
8		acidic chitinase III	0.1	0.00272
9	R-112_C(	70 kDa heat shock protein [Chlamydomonas reinhardtii]	0.072	0.62039
10	R-038_A1	lipoxygenase [Nicotiana attenuata]	0.28	0.00193
11	R-040_b1	lipoxygenase [Nicotiana attenuata]	0.17	0.03572
12	R-120_C1	isoflavone reductase-like protein [Nicotiana sylvestris]	0.17	0.0284
13	NM-18-3	AAA protein	0.27	0.00253
14	l-012_a01	Oxygen-evolving enhancer protein 1	0.11	0.03355
15	L-077_H	ethylene-inducible protein	0.51	0.04817
16	l-012_c01	33kDa precursor protein of oxygen-evolving complex [Solanum tuberos	0.12	0.0284
17	L-038_F0	Np-ypt3 [Nicotiana plumbaginifolia]	0.3	0.03568
18	R-124_C1	germin-like protein [Lycopersicon esculentum]	0.06	0.00253
19	GRP		0.06	0.03355
20	l-032_c12	WD40-repeat protein [Arabidopsis thaliana]	0.14	0.04962
21	l-088_e03	thionin like protein [Nicotiana tabacum]	0.19	0.0399
22	l-003_e04	thionin like protein [Nicotiana tabacum]	0.01	0.00244
transporte/6				
1	l-084_e02	putative sugar transporter protein [Oryza sativa (japonica cultivar-group	0.01	0.00104
2	R-083_F0	amino acid transporter [Lycopersicon esculentum]	0.06	0.02949
3	L-065_B(	sucrose transporter [Nicotiana tabacum]	0.12	0.0335
4	l-024_g1(	utative golgi transport complex protein; 67058-70172 [Arabidopsis thal	0.3	0.03104
5	R-031_b0	Similar to nitrate and oligopeptide transporters [Arabidopsis thaliana]	0.11	0.03208
6	l-023_a06	vacuolar processing enzyme-3 [Nicotiana tabacum]	0.26	0.001
cell structure/11				
1	R-125_E(	alpha-tubulin [Streblomastix strix]		
2	R-046_H1	proline-rich protein family [Arabidopsis thaliana]	0.14	0.003
3	R-078_F1	putative hydroxyproline-rich glycoprotein [Oryza sativa (japonica cultiv	0.04	0.03498
4	l-106_f07	major intrinsic protein 1 [Solanum tuberosum]	0.3	0.04829
5	l-127_d0	Putative integral membrane protein [Arabidopsis thaliana]	0.19	0.05423
6	R-020_F0	actin-depolymerizing factor 2 [Petunia x hybrida]	0.22	0.0477
7	R-040_b0	fiber protein Fb11 [Gossypium barbadense]	0.24	0.03865
8	R-057_a0	endosperm-specific protein-like protein [Arabidopsis thaliana]	0.17	0.03298
9	R-020_B(	putative coatomer protein gamma 2-subunit [Oryza sativa (japonica cul	0.15	0.00061
10	l-108_d04	endoxyloglucan transferase [Daucus carota]	0.25	0.03896
11	l-107_a1(	putative microtubule-associated protein [Arabidopsis thaliana]	0.07	0.03104
protein distribution and stoge/10				
1	R-117_D03	putative protein kinase [Arabidopsis thaliana]	0.21	0.00482
2	l-093_c01	proteasome alpha subunit [Petunia x hybrida]	0.19	0.04676
3	R-101_f0	putative alpha3 proteasome subunit [Nicotiana tabacum]	0.27	0.03348
4	l-089_h06	aspartic proteinase 2 [Glycine max]	0.08	0.00039
5	l-057_g07	putative serine/threonine kinase [Oryza sativa (japonica cultivar-group)]	0.01	0.0284
6	l-058_c07	carbohydrate kinase-like protein [Arabidopsis thaliana]	0.15	0.05423
7	R-074_D(	putative chaperonin gamma chain [Arabidopsis thaliana]	0.1	0.00335
8	R-104_D(	putative ubiquitin-specific protease [Oryza sativa (japonica cultivar-gro	0.18	0.05423
9	L-078_D(	mitochondrial Lon protease homolog 1 precursor [Arabidopsis thaliana]	0.15	0.06525
10	R-031_f0	putative FtsH protease [Oryza sativa (japonica cultivar-group)]	0.14	0.00386
transciption/21				
1	R-063_D08	elongation factor 1B gamma [Oryza sativa]	0.01	0.03821
2	R-121_A01	bHLH transcriptional regulator [Lycopersicon esculentum]	0.09	0.01228
3	R-086_G07	putative exonuclease RRP41 [Arabidopsis thaliana]	0.25	0.04694
4	l-	telomere binding protein TBP1 [Nicotiana glutinosa]	0.11	0.05043
5	l-	putative C2H2-type zinc finger protein [Arabidopsis thaliana]	0.28	0.03275

6	L-064_E08	isoleucine-tRNA ligase - like protein [Arabidopsis thaliana]	0.19	0.04284
7	L-100_a1	transcription factor LIM [Nicotiana tabacum]	0.08	0.03751
8	R-002_E(	Putative CAF protein [Oryza sativa (japonica cultivar-group)]	0.12	0.04633
9	L-066_D(	nucleic acid binding protein-like [Arabidopsis thaliana]	0.18	0.03208
10	l-106_e02	poly(A) polymerase [Pisum sativum]	0.3	0.04108
11	l-094_f11	putative small nuclear ribonucleoprotein Prp4p [Arabidopsis thaliana]	0.19	0.05726
12	l-012_b04	putative ribosomal protein L18 [Arabidopsis thaliana]	0.09	0.0399
13	R-103_b0	Putative splicing factor Prp8 [Arabidopsis thaliana]	0.23	0.04724
14	R-098_H(	putative DEAD/DEAH box RNA helicase protein [Arabidopsis thaliana	0.17	0.03237
15	R-062_C1	putative pre-mRNA splicing factor PRP19 [Arabidopsis thaliana]	0.21	0.00241
16	l-017_a01	DEAD-Box RNA helicase-like protein [Arabidopsis thaliana]	0.3	0.09105
17	R-065_g1	multifunctional aminoacyl-tRNA ligase-like protein [Arabidopsis thalia	0.21	0.04962
18	R-056_H1	putative lipase [Arabidopsis thaliana]	0.17	0.0587
19	l-	mRNA-binding protein precursor [Nicotiana tabacum]	0.16	0.03208
20	R-001_g0	putative RNA helicase [Arabidopsis thaliana]	0.28	0.02916
21	l-105_c11	elongation factor EF-2 [Arabidopsis thaliana]	0.19	0.01512

sinal transduction/2

1	R-077_C1	Probable microsomal signal peptidase 12 kDa subunit (EC -related [Ara	0.21	0.04633
2	L-097_F0	putative EBNA1-binding protein homolog; Ebp2p [Oryza sativa (japoni	0.37	0.47585

secondary metaboli:/5

1	l-106_d03	Ubiquitin conjugating enzyme [Cicer arietinum]	0.26	0.03467
2	L-014_h0	polyubiquitin [Pinus sylvestris]	0.26	0.06016
3	l-092_c1	putative C-4 sterol methyl oxidase [Arabidopsis thaliana]	0.15	0.09674
4	R-012_a0	flavonoid O-methyltransferase [Catharanthus roseus]	0.19	0.01476
5	l-012_e07	squalene synthase [Nicotiana tabacum]	0.21	0.04716

cell cycle:/0

metabolis./29

1	R-001_f11	putative phosphatidylglycerolphosphate synthase [Oryza sativa (japonic	0.31	0.03805
2	L-046_G06	chorismate mutase [Arabidopsis thaliana]	0.25	0.00223
3	R-015_b0	kinesin-like protein A, putative [Arabidopsis thaliana]	0.03	0.00987
4	L-005_F12	probable [acyl-carrier-protein] S-malonyltransferase (EC 2.3.1.39) T27	0.01	0.05101
5	R-041_E(	homocysteine S-methyltransferase AtHMT-2 [Arabidopsis thaliana]	0.34	0.09778
6	l-086_e06	GTP-binding membrane protein LepA homolog [Arabidopsis thaliana]	0.24	0.04596
7	L-020_B(	putative GTP-binding protein [Cucumis sativus]	0.15	0.04015
8	R-036_G(	putative calcium channel [Arabidopsis thaliana]	0.3	0.03799
9	R-069_d0	cytosolic cysteine synthase [Solanum tuberosum]	0.27	0.03414
10	l-012_a04	putative serine carboxypeptidase II-like protein [Oryza sativa (japonica	0.25	0.03275
11	R-125_D1	glycolate oxidase [Lycopersicon esculentum]	0.13	0.03013
12	l-103_h11	NADPH:protochlorophyllide oxidoreductase [Nicotiana tabacum]	0.06	0.07421
13	R-094_F0	protoporphyrinogen oxidase PX-2 [Nicotiana tabacum]	0.35	0.01014
14	l-034_g11	Mg protoporphyrin IX chelatase [Nicotiana tabacum]	0.3	0.03618
15	R-004_d0	progesterone 5-beta-reductase [Digitalis purpurea]	0.2	0.02861
16	R-092_F08	LAX1 / AUX1-like permease [Arabidopsis thaliana]	0.03	0.0284
17	R-044_B09	GAST-like gene product [Fragaria x ananassa]	0.04	0.04633
18	L-017_G(	cytosolic NADP-malic enzyme [Lycopersicon esculentum]	0.16	0.0318
19	R-003_a0	ubiquinol--cytochrome c reductase [Solanum tuberosum]	0.36	0.09552
20	.R-034_F(	geraniol 10-hydroxylase [Catharanthus roseus]	0.24	0.04505
21	wFAD		0.13	0.00193
22	L-041_H(	purple acid phosphatase [Nicotiana tabacum]	0.1	0.02101
23	l-086_f12	extracellular calcium sensing receptor [Arabidopsis thaliana]	0.31	0.05171
24	R-010_e1	putative serine carboxypeptidase [Oryza sativa (japonica cultivar-group	0.03	0.03739
25	R-020_D1	catechol O-methyltransferase [Nicotiana tabacum]	0.12	0.00987

26	L-008_G(	UDP-glucose:protein transglucosylase [Solanum tuberosum]	0.34	0.27437
27	R-008_a0	putative PHD-type zinc finger protein [Arabidopsis thaliana]	0.04	0.00193
28	l-026_d0	hydroxymethylglutaryl coenzyme A synthase [Hevea brasiliensis]	0.38	0.08251
29	l-015_a0	putative RING zinc finger ankyrin protein [Arabidopsis thaliana]	0.18	0.05101

energy/14

1	l-	chlorophyll a/b binding protein [Nicotiana tabacum]	0.12	0.06385
2	L-097_C1	chlorophyll a/b binding protein [Petunia x hybrida]	0.1	0.977
3	R-123_G09	cytochrome P450 CYP74C3 [Lycopersicon esculentum]	0.31	0.03996
4	l-057_f03	light-harvesting chlorophyll a /b binding protein [Nicotiana tabacum]	0.22	0.0354
5	L-097_D(	chlorophyll a/b-binding protein (cab-12) - tomato	0.18	0.04964
6	l-092_f05	utative chlorophyll A-B binding protein of LHCII type III, [Oryza sativa	0.01	0.03702
7	L-086_E0	photosystem I reaction center subunit X psaK [Nicotiana tabacum]	0.12	0.03237
8	l-017_g01	light-harvesting chlorophyll a /b binding protein [Nicotiana tabacum]	0.34	0.09879
9	R-106_E(	mitochondrial ATPase beta subunit [Nicotiana sylvestris]	0.14	0.05731
10	L-007_C(	putative chlorophyll A-B binding protein type I [Pinus pinaster]	0.17	0.04738
11	l-057_c04	light-harvesting chlorophyll a /b binding protein [Nicotiana tabacum]	0.27	0.03651
12	-088_c05	light harvesting chlorophyll a/b-binding protein [Nicotiana sylvestris]	0.2	0.05161
13	R-101_a0	Cryptochrome 1b [Lycopersicon esculentum]	0.14	0.00508
14	l-104_g07	photosystem I light-harvesting chlorophyll a/b-binding protein [Nicotiar	0.13	0.00928

others/43

1	l-024_d0	unnamed protein product [Nicotiana tabacum]	0.21	0.06381
2	l-089_a0	ribosomal protein L11-like protein [Arabidopsis thaliana]	0.28	0.00429
3	L-079_C(	expressed protein [Arabidopsis thaliana]	0.26	0.04485
4	R-115_H	5.8 kb basic protein [Phaseolus vulgaris]	0.2	0.03944
5	L-054_B(	water channel-like protein [Arabidopsis thaliana]	0.01	0.03618
6	l-104_d11	SPP30 [Solanum chacoense]	0.18	0.04946
7	R-010_b0	pheromone receptor, putative (AR401) [Arabidopsis thaliana]	0.29	0.06723
8	R-123_H(	putative carrier protein [Arabidopsis thaliana]	0.31	0.063
9	l-109_d0	Putative amp-binding protein [Arabidopsis thaliana]	0.11	0.04608
10	R-001_f0	P69C protein [Lycopersicon esculentum]	0.16	0.00152
11	L-103_e0	ribosomal protein L23a [Fritillaria agrestis]	0.1	0.03348
12	L-103_C(	NtpII10 [Nicotiana tabacum]	0.08	0.03237
13	R-018_G	putative urease accessory protein F [Lycopersicon esculentum]	0.17	0.00551
14	R-078_G	putative AtHVA22a protein [Arabidopsis thaliana]	0.17	0.03726
15	R-115_F0	putative ribosomal protein S29 [Oryza sativa (japonica cultivar-group)]	0.11	0.02127
16	l-093_d0	putative inward rectifying potassium channel [Solanum tuberosum]	0.24	0.03237
17	R-095_C(	histone H3	0.25	0.00884
18	l-002_h0	succinate dehydrogenase iron-sulfur protein subunit [Cucumis sativus]	0.04	0.02029
19	l-087_h01	histone H2A:ISOTYPE=9	0.05	0.03572
20	R-101_a1	homeobox gene [Nicotiana tabacum]	0.31	0.03467
21	l-090_c11	starch (bacterial glycogen) synthase [Solanum tuberosum]	0.33	0.04485
22	l-068_f12	ribonuclease NGR2 [Nicotiana glutinosa]	0.36	0.08948
23	R-057_c1	RNA-binding glycine-rich protein-1 (RGP-1a) [Nicotiana sylvestris]	0.06	0.02262
24	L-014_a1	SLL2-S9-protein [Brassica rapa]	0.23	0.01815
25	R-103_e0	F12A21.11 [Arabidopsis thaliana]	0.32	0.04307
26	R-092_B(	pollen-related protein -related [Arabidopsis thaliana]	0.19	0.05364
27	R-115_H	class II knotted-like homeodomain protein [Lycopersicon esculentum]	0.31	0.02161
28	L-010_h1	putative peptide chain release factor subunit 1 (ERF1) [Oryza sativa (ja	0.38	0.01606
29	l-017_b0	putative leaf development protein Argonaute [Arabidopsis thaliana]	0.07	0.0935
30	l-062_a1	plastid ribosomal protein S9 precursor [Spinacia oleracea]	0.15	0.05225
31	O19-C-1		0.31	0.01922
32	l-074_c11	potassium channel [Nicotiana paniculata]	0.01	0.0416
33	l-001_e01	putative ripening-related protein [Vitis vinifera]	0.11	0.0081
34	l-027_h0	ripening-related protein-like [Arabidopsis thaliana]	0.34	0.21342
35	L-080_G(	alcohol dehydrogenase [Petunia x hybrida]	0.15	0.04044
36	L-102_b0	6b-interacting protein 1 [Nicotiana tabacum]	0.32	0.07961
37	R-064_e1	GCN4-complementing protein (GCP1) [Arabidopsis thaliana]	0.01	0.00955

38	l-108_e05	PP2A regulatory subunit-like protein [Oryza sativa (japonica cultivar-g	0.18	0.03312
39	R-035_F0	putative trehalose-6-phosphate phosphatase (AtTPPA) [Arabidopsis tha	0.17	0.00979
40	l-094_c07	transformer-SR ribonucleoprotein [Nicotiana tabacum]	0.21	0.04771
41	l-105_h08	synaptobrevin-like protein [Arabidopsis thaliana]	0.34	0.03805
42	R-121_B0	putative ring box-1 protein [Oryza sativa (japonica cultivar-group)]	0.34	0.03799
43	l-103_g07	ribosomal protein L23a [Fritillaria agrestis]	0.12	0.68376

unkown/76

1	l-093_a01
2	R-040_h08
3	R-032_C01
4	R-019_A02
5	L-046_E09
6	R-006_b06
7	L-006_G02
8	R-057_e01
9	L-048_D09
10	L-010_b11
11	l-084_c07
12	L-035_B06
13	L-098_b08
14	l-092_f01
15	R-030_g12
16	R-101_c12
17	L-079_C02
18	R-003_f11
19	l-012_d10
20	l-093_e01
21	l-093_g05
22	l-024_a08
23	l-057_c07
24	L-010_g05
25	l-057_g11
26	l-072_e03
27	L-097_B09
28	l-088_a07
29	l-029_c05
30	R-063_A05
31	l-033_g12
32	R-018_C05
33	l-106_f08
34	l-105_a11
35	l-022_a11
36	R-066_c06
37	L-014_c09
38	R-106_B09
39	L-098_f01
40	R-019_H03
41	R-119_D04
42	l-070_d03
43	R-056_F07
44	l-062_f05

45 l-086_a03
46 l-057_e01
47 l-012_e05
48 R-076_G02
49 L-049_C05
50 L-102_d05
51 l-105_c09
52 R-021_D03
53 l-093_e07
54 R-004_g09
55 R-028_B05
56 R-026_E02
57 l-056_d02
58 l-001_a09
59 L-046_B10
60 R-014_H10
61 l-033_d05
62 R-123_G12
63 R-079_G11
64 R-101_a07
65 R-059_B05
66 l-022_b12
67 R-011_b07
68 R-097_C03
69 L-044_A01
70 l-002_g02
71 l-057_g01
72 L-096_e07
73 R-100_h11
74 l-087_b03
75 L-038_G08
76 l-094_b12